

STUDY ON SHAPE SEPARATION OF PARTICULATE MATERIALS

大矢, 仁史

<https://doi.org/10.11501/3132443>

出版情報 : 九州大学, 1997, 博士 (工学), 論文博士
バージョン :
権利関係 :

STUDY ON SHAPE SEPARATION
OF PARTICULATE MATERIALS

(粒子状物質の形状分離に関する研究)

Hitoshi OHYA

①

STUDY ON SHAPE SEPARATION OF PARTICULATE MATERIALS

1997. 11.

Hitoshi OHYA
Materials Handling and Characterization Laboratory
Materials Processing Department
National Institute for Resources and Environment, MITI

Chapter 1. Introduction	1
1.1 General introduction	1
1.2 Expression of particle shape	6
1.3 Application of particle shape separation	10
1.4 Current developments on particle shape separation	12
1.5 Order of presentation	27
Chapter 2. Inclined vibration plate	28
2.1 Introduction	28
2.2 Theory on trajectory of particles	30
2.3 Accurate shape sorting of glass beads and sands	34
2.4 Conclusions	43
Chapter 3. Horizontally circular motion plate	44
3.1 Introduction	44
3.2 Analysis of the particle movement	46
3.3 Separation performance for spherical glass beads and nonspherical ground glass powders	55
3.4 Shape separation for fine particles	66
3.5 Distinction of nonspherical particles	68
3.6 Conclusions	74
Chapter 4. Inclined conveyor	75
4.1 Introduction	75
4.2 Theory on trajectory of particles	77
4.3 Comparison of experimentally collected position with calculated trajectory	85
4.4 Conclusions	100

Chapter 1. INTRODUCTION

Chapter 5. Recovery of reclaimed foundry sands with inclined conveyor	101
5.1 Introduction	101
5.2 Separation and recovery performance of advanced foundry sands	104
5.3 Improvement of feeding and abundance fraction	108
5.4 Conclusions	116
Chapter 6. Application of recycling using particle shape separation	117
6.1 Introduction	117
6.2 Pretreatment of a scrapped electronic appliance	118
6.3 Recovery of copper from printed wiring board	126
6.4 Conclusions	138
Chapter 7. Summary and conclusions	139
Appendix	142
Nomenclature	144
Acknowledgments	147
References	149

Chapter 1. INTRODUCTION

1.1 General introduction

The current development stage of renewable energy sources and various political, economic and environmental factors have until now dictated the use of fossil fuels as a major energy source well into the next century.

On the other hand, we have a developed and comfortable civilization. It is supported by mass production and consumption. We have to change our life style to keep a sustainable development measured against the problems of the global environment[1-3].

The industrial activities that support society and the activities of our everyday life are the source of quite a remarkable amount of waste. In fact, it is estimated that the total amount of waste generated in 1990 by manufacturing industries in Japan amounted to as much as 243,220,000 tons.

In addition to this, the amount of general domestic wastes generated from households and other sources showed a steady increase of three or four percent a year since 1985, until it reached a total of 49,970,000 tons in 1991.

The processing plants and waste disposal sites are now reaching the point where they can no longer keep up with the ever increasing quantity of waste, and we now find ourselves in a position where we must either come up with a way to immediately reduce our total amount of waste or else face increasingly serious environmental problems. The addition to this, the cost to the average citizen for dealing with these wastes is yearly rising; therefore, this makes the rapid reduction in the amount of garbage we generate essential to the maintenance of a strong and healthy economy as well.

While, on the one hand, Japan has come to be known as an economic superpower, it is also one of the few nations in the world which may be counted as a net consumer of resources. Also, Japan must rely on imports from overseas for a large part of

these resources. If our nation is to continue following the path of a stable and rich life for everyone, then we must begin to give serious thought to using the limited resources of the Earth more wisely.

Many other countries in the world have the same social problems. Japan seems to be a small model of the world for resource recycling.

Figure 1.1 shows how the waste generated in 1990 by manufacturing industries throughout Japan were processed or recycled.

The total amount of industrial waste generated can be divided into three categories:

1. Waste processed immediately (18,663 million tons)
2. Waste immediately recycled as resource (68,134 million tons)
3. Waste subjected to burning, drying or some other form of intermediate waste processing (156,425 million tons)

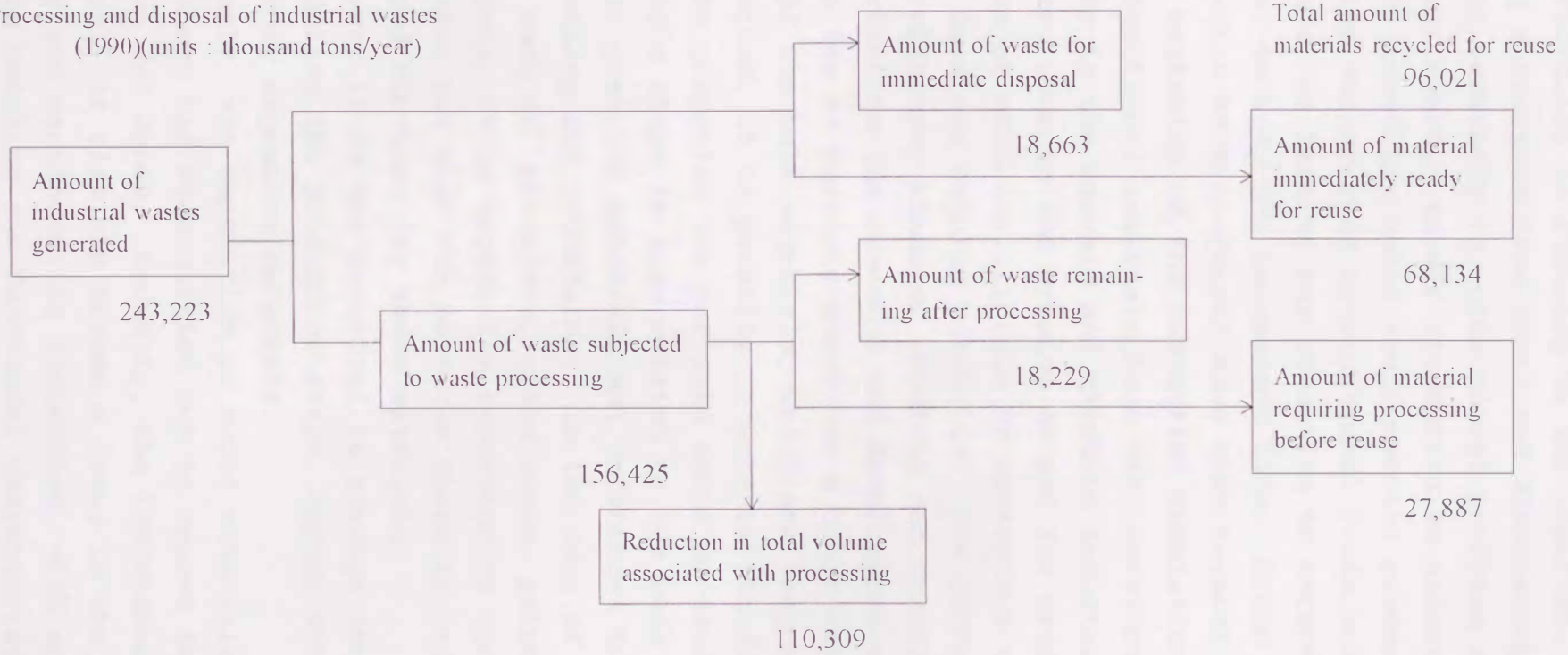
Waste management systems are important for resource recycling, but at the core of these systems, we, the researchers, have to think about a good process in this technology field. The outline for resource recycling is

1. Research on waste characterization
2. Size reduction and handling before separation
3. Physical separation (density separation, size classification, electrostatic separation,)
4. Physical-chemical separation (flotation,)
5. Chemical separation (leaching, extraction,)

The numbers of process steps depend on the cost of the recycled materials. Processed 1 to 3 should be used for most of the generated industrial waste.

In the field of technology, mining engineering and chemical engineering have been changing and searching for new research subjects and applications. We do not develop any more mines in Japan. However, their technologies are applicable to the separation of waste[4-5].

Processing and disposal of industrial wastes
(1990)(units : thousand tons/year)



(from MITI survey)

Fig.1.1 Processing and disposal of industrial waste

Nanjo[6] calls it the urban mine instead of a real mine. Resource recycling is focusing on the important technology of recovering a resource from waste and diminishing the waste volume. It is necessary to solve social problems and maintain the global environment. We are attempting to undertake a big national project, named the total environmental process of zero emission, by the Ministry of International Trade and Industry.

In fact, we have to pay attention to recent research and development to keep our convenient life. Gross net product and the population have increased more than several hundred times since the beginning of the industrial revolution.

New functional materials have been developed into a variety of products in the ceramic and electric industries over the last few decades. Due to the growing demand for products with a very high degree of accuracy, fibrous or membranous materials rather than bulk ones are gaining attention. The production of fine particles with many kinds of physical and chemical properties is very important in the research and development of new materials.

In so far as particle shape has a close relationship to the function of the bulk materials, which are composed of the particles concerned, it is possible to enhance the function of the material by preparing the particle shape as desired[7].

Particle shape is also related to the bulk properties of powdered or granular materials and influences their behavior during handling and processing. In the case of particulate materials such as abrasives, glass beads, paints, foundry sands and catalysts, it is especially important to control not only particle size but also the particle shape in order to bring about the required function for these materials.

However, it is not practical to arrange the shape of every particle during the production stage, except for some special cases of very expensive materials.

Formerly, the separation of solid materials according to particle shape had been carried out to remove foreign materials from grains and seeds. Recently, the importance of particle shape as well as size has become a focus in the chemical, mineral processing and manufacturing industries, with an eye to improvement in the handling and functional characteristics of particu-

late materials.

Generally speaking, the word "classification" means the separation technique by size in the fields of mining and chemical engineering. At least, we often recognized it as such. But "classification" just means the separation of some parts on purpose. This means that most of the separation performed is size separation. Sometimes gravitational and shape separation is necessary to establish a good development of the product.

Focus on the shape is needed, for example, in spherical particles for ceramics, powder metallurgy, casting sand, solder beads and toner carrier; angular particles for abrasives, needle form of iron oxide for magnetic recording, needle form of titan dioxide for paints preventing electrostatic loading, and flattened particles for cosmetics and pigments.

Shape separation can be applied not only to the development of materials, but also to recycling. Currently, particle shape separation or classification must become an important technique to maintain a good environment and develop functional materials.

It is important to control the particle shape, but in the literature, there are not many studies on this subject. In this report, current developments and investigations of particle shape separation are described.

1.2 Expression of particle shape

Before shape separation, it is necessary to grasp particle shapes quantitatively[8]. We note that most expressions of particle shapes would not mean a geometrical description, but an irregular form. Some descriptive terms are shown in Table 1.1.

The quantitative approach results in using a shape index or a shape factor which appeared in the paper written by Endoh[9]. A shape factor is physical or geometrical gap compared with a sphere. A shape index is the direct explanation of the geometrical shape.

It is very important for particle shape separation to focus on the particle characterization depended on the shape. We want to propose which factor or index is the most effective to estimate separation results. In this section, we can see an example of a shape index and shape factor in Tables 1.2 and 1.3, respectively.

Table 1.1 Descriptive terms on particle shape

spherical	sponge
cubical	blocky
prismoidal	sharp edged
platy	rounded
flake-like, flaky	porous
granular	agglomerate
rod-like	hollow
needle-like, acicular	rough
fibrous	smoothed
dendritic	fluffy, nappy

Table 1.2 Shape index

proportion	$CAR = D_R(\theta_{max})/D_R(\theta_{max} + \pi/2)$ elongation: $Z = l/b$ flakiness = b/t Zigg's index: $F = Z/(b/t) = lt/b^2$ anisometry: $K = (I_1/I_2)^{1/2}$	θ_{max} : θ at maximum D_R l : length, b : breadth, t : thickness I_1, I_2 : principle moment of inertia
degree of sufficiency space	degree of volume sufficiency $fv = lbt/V$ Schulz's index: $k = nl^2b - 100$ Hager's index: $fs = (l/t)fv$ bulkiness index: $f_b = A/A'$ bulkiness: $B = 4\pi R_1R_2/A$	V : volume of particle $n = 100/V$ A : projected area of particle A' : area of the minimum rectangle circumscribed with the project figure $R_i : (I_i/A)^{1/2}$
degree of true sphericity and circularity	degree of true sphericity $\psi_s = S_{sp}/S$ Wadell's sphericity: $\psi_w = D_H/D_{min}$ Aschenbrenner's sphericity degree of circularity $\psi_{HL} = Lc/L = D_H/D_L$ $\psi_{RL} = \overline{D_R}/D_L, \psi_{RH} = \overline{D_R}/D_H$	S : surface area, $S_{sp} = 4\pi(6V/\pi)^{2/3}$ L : perimeter D_{min} : diameter of the minimum circle circumscribed with the projected figure D_H : Heywood diameter = $(4A/\pi)^{1/2}$ $Lc: \pi D_H, D_L = L/\pi$ mean expand diameter: $\overline{D_R} = \int_0^\pi D_R(\theta)d\theta/\pi$
degree of circularity	roundness $\Sigma\rho_i/NR_{max}$ surface factor: $L^2/12.6A = 1/\psi_{HL}^2$ degree of concave $\psi_{FL} = \overline{D_F}/D_L$ rugosity	σ_1 = local by the arc curvature contours approximated N : number of approximate arc, R_{max} : radius of maximum inscribed circle mean Feret diameter: $\overline{D_F} = \int_0^\pi D_F(\theta)d\theta/\pi$
	variation coefficient of expand diameter σ_R variation coefficient of Feret diameter σ_F	$\sigma_S = [\int_0^\pi \{D_S(\theta) - D_S\}^2 d\theta]^{1/2} / D_S$ subscript S: F or R
Fourier descriptor	Fourier spectrum A_k, a_k polar coordinate method $A_k^* = A_k/A_0$ $IRP = (D_H/2A_0)^2 = 1/\psi_{RH}^2$ Randiance = $\mu_2/A_0^2 = \Sigma A_k$ Skewness = μ_3/A_0^3 Particle Signature	polar coordinate method ($r(\theta)$), amplitude method ($\phi^*(t)$), $r(s)$ method, method of distance from centroid, r : distance from centroid, $\phi^*(t)$: amplitude, s : arc length, $t = 2\pi s/L$, $A_k^2 = Ck ^2$ α_k : aggregated sampling angle $C_k = (a_k - jb_k)/2 = \int_0^{2\pi} F(\theta)\exp(-jk\theta)d\theta/2\pi$ $\mu_m = \int_0^{2\pi} \{r(\theta) - A_0\}^m d\theta/2\pi$

Table 1.3 Shape factor

	name of factor	definition	relation
geometric shape factor	surface shape factor	$\phi_s = S/D_p^2$	$\phi_s = \pi$ at $D_p = D_H$
	volume shape factor	$\phi_v = V/D_p^3$	$\phi_v = \pi/6$ at $D_p = D_v$
	specific surface shape factor	$\phi_{sv} = (S/V)D_p = S_v D_p = \rho_p S_w D_p$	$\phi_{sv} = \phi_s / \phi_v$
	Carman's shape factor	$\phi_c = 6 / \phi_{sv}$	
dynamics shape factor	resistance shape factor	$K_R = R / 3\pi\eta v D_p$	$D_p = D_e, K_R = K_{Rv} = v_{sp}/v$
	kinetics shape factor	$\kappa = \frac{\text{actual } R \text{ forced to particle}}{\text{R forced to sphere having the same volume}}$	$D_p = D_e, \kappa = K_{Rv}, \kappa = (D_e/D_{st})^2$ when particles are agglomerated, $\kappa = (D/D_{agst})^2 (1-\epsilon)^{-1}$

S : surface area of particle, V : volume of particle, D_H : Heywood diameter, D_e : sphere equivalent diameter, D_{st} : Stokes diameter

1.3 Application of particle shape separation

Classification has been in terms of size until now, but it is clear that the notion of different shapes of the same size will be related to the characterization of particulate materials. Because the demand for solid materials requires a high degree of accuracy, shape characterization will become connected to the accuracy of those materials.

From this point of view, the current technique is for studying coarse particles, but fine particles and powders will remain an important target in the field of this investigation in the future.

Particle shape separation yields not only high additional values to materials but also has significant meaning for the investigation of powder technology. Advancement in this field is greatly anticipated.

Table 1.4 Application for shape separation

Material	Shape	Characteristics
Toner Carrier Ceramics, Powder Metallurgy Solder Beads Casting Sand Abrasives Iron Oxide for Recording Titan Dioxide for paints Cosmetics, Pigment	Spherical Spherical Spherical Spherical Angular Needle-like Needle-like Flattened	Clear Copy Close Packing Precise Print Flowability Effective Abrasion Magnetic Characterization Electric Loading Luster

1.4 Current development in particle shape separation

1.4.1 Assortment of Shape Separators

Characterization values of the particle shape must be considered when the shape separation technique is applied. The values concern such factors as sliding or rolling character, passing rate through a sieve and adhesive force[10-12]. Table 1.5 shows the assortment of this technique according to these principles.

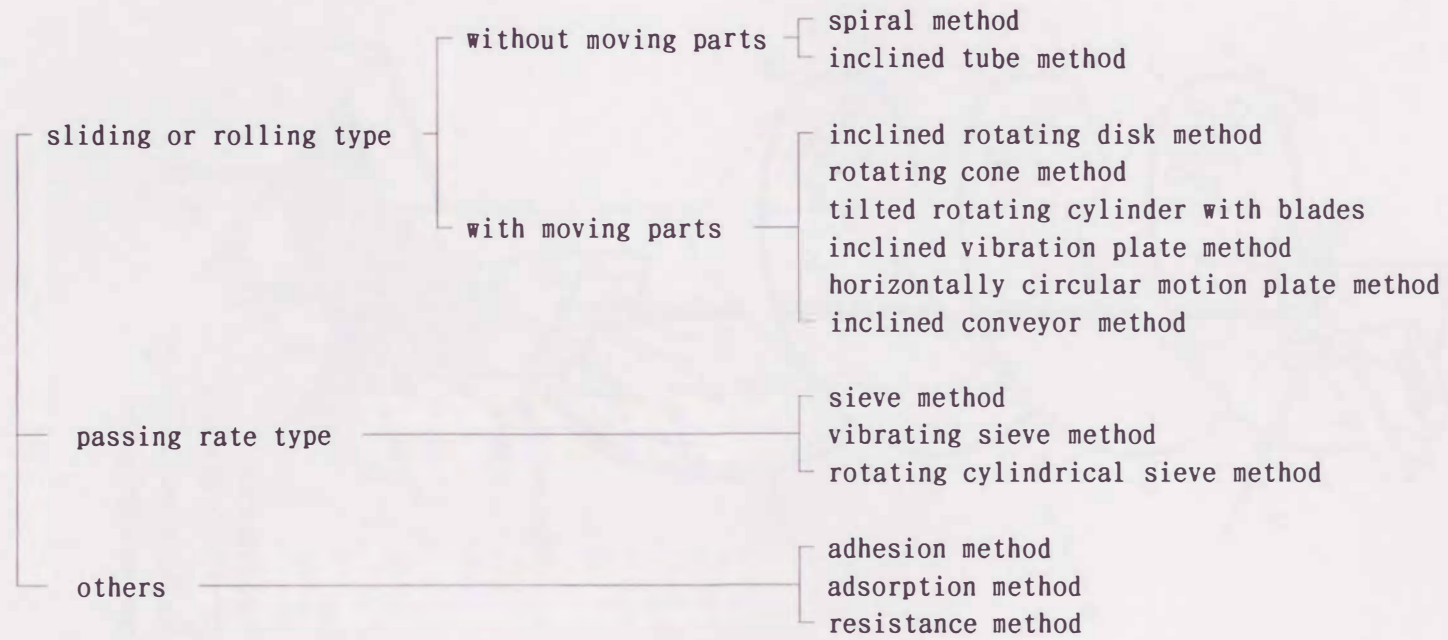
1.4.2 Sliding or Rolling Type

Most of the apparatuses selected are belonging to sliding or rolling type, and many papers and patents are available. First, Berensford's instrument[13] was elaborated for a particle shape separator without a moving part. As shown in Fig. 1.2, it had a spiral plate on which the particles rolled down with only gravity. Spherical particles were collected in an outside vessel because the spherical shapes ran down faster than the nonspherical ones. Glezen and Ludwich's inclined chutes[14] were based on the same concept (see Fig. 1.3). It consisted of two long chutes which were inclined at different angles and three collected containers. Waldie[15] separated glass from river sand using a rotating cylinder, instead of the chutes, in the same manner as Glezen and Ludwich.

Second, the inclined rotating disk method was most famous among sliding or rolling type separators with moving parts. This method was developed by Thompson[16] in 1907. Prinz[17], Lotzky[18], and Ulrich[19] published similar reports. Carpenter and Deits[20], Riley[21], Klar[22] et al. studied this method in detail; it was based on the principle of different trajectories on which spherical particles rolled down in the direction of the inclined disk to have nothing to do with the disk rotation but nonspherical particles were carried out by the rotation.

Riley separated spherical, cylindrical, platy and irregular grains made of glass using the apparatus shown in Fig. 1.5.

Table 1.5 Assortment of shape separators



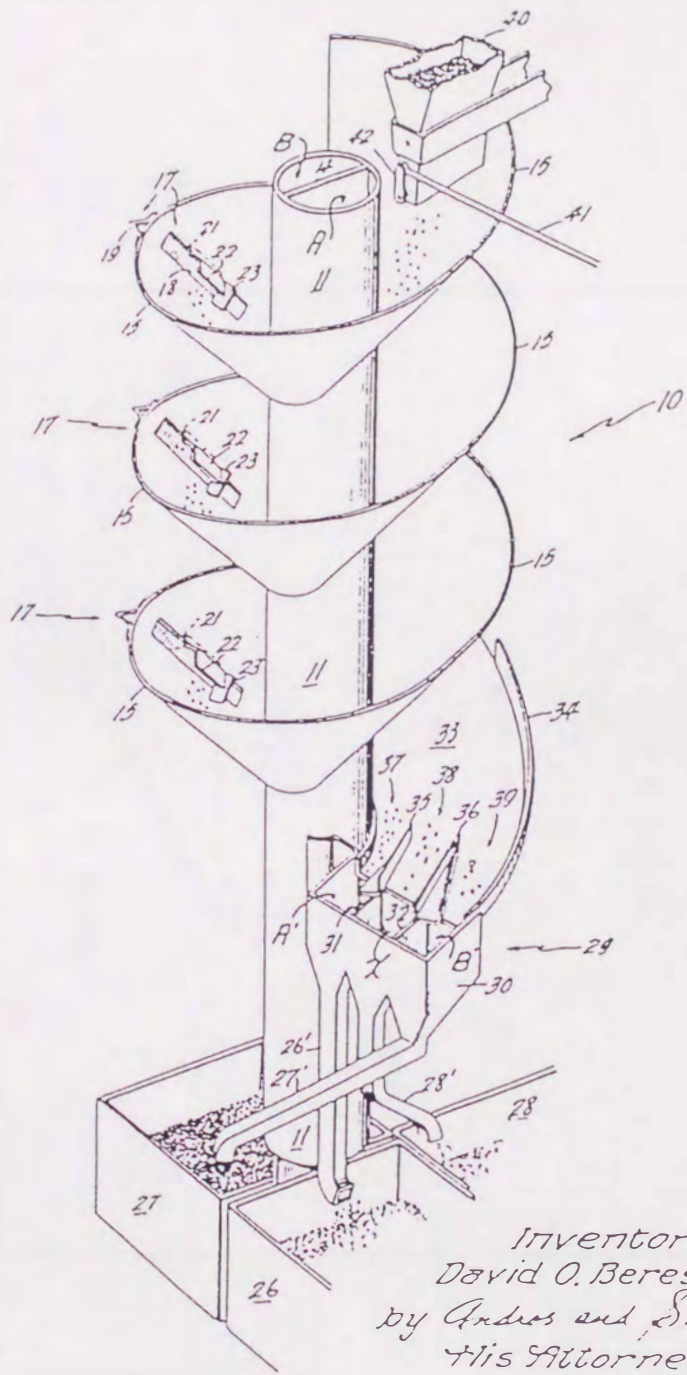


Fig.1.2 Spiral method

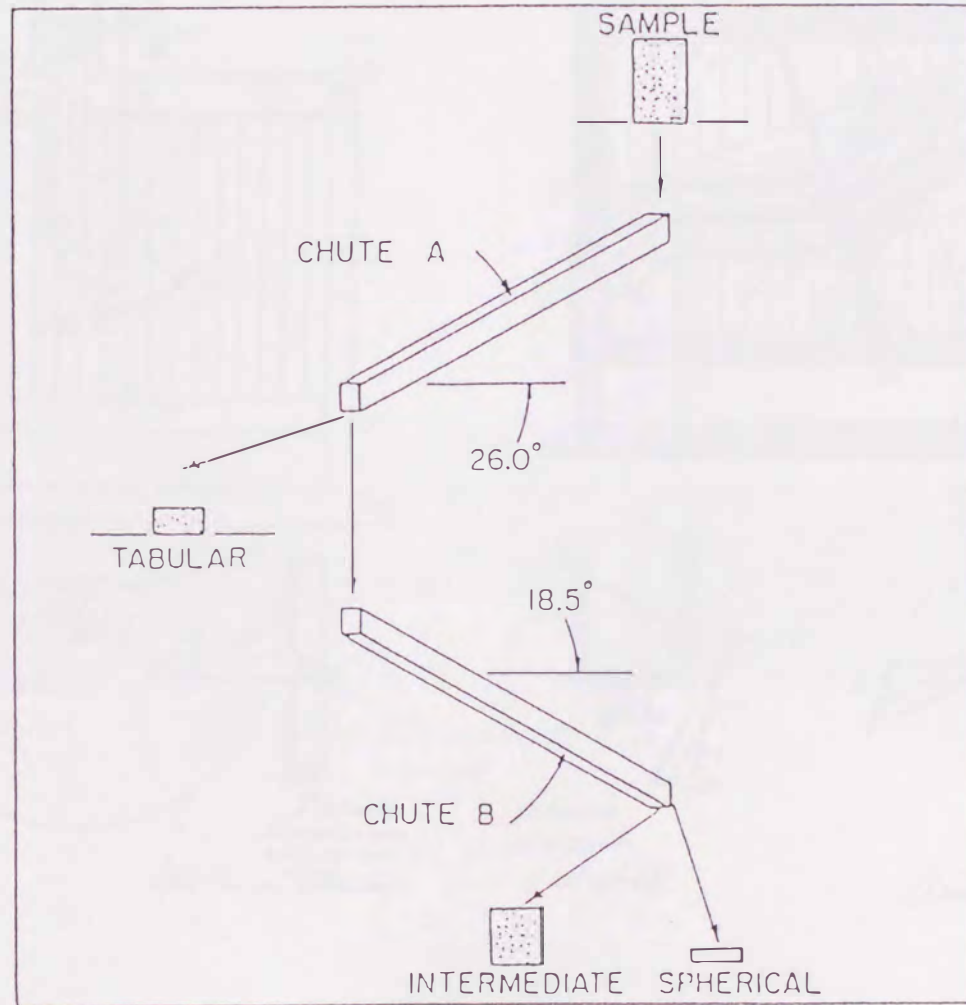


Fig.1.3 Inclined chute method

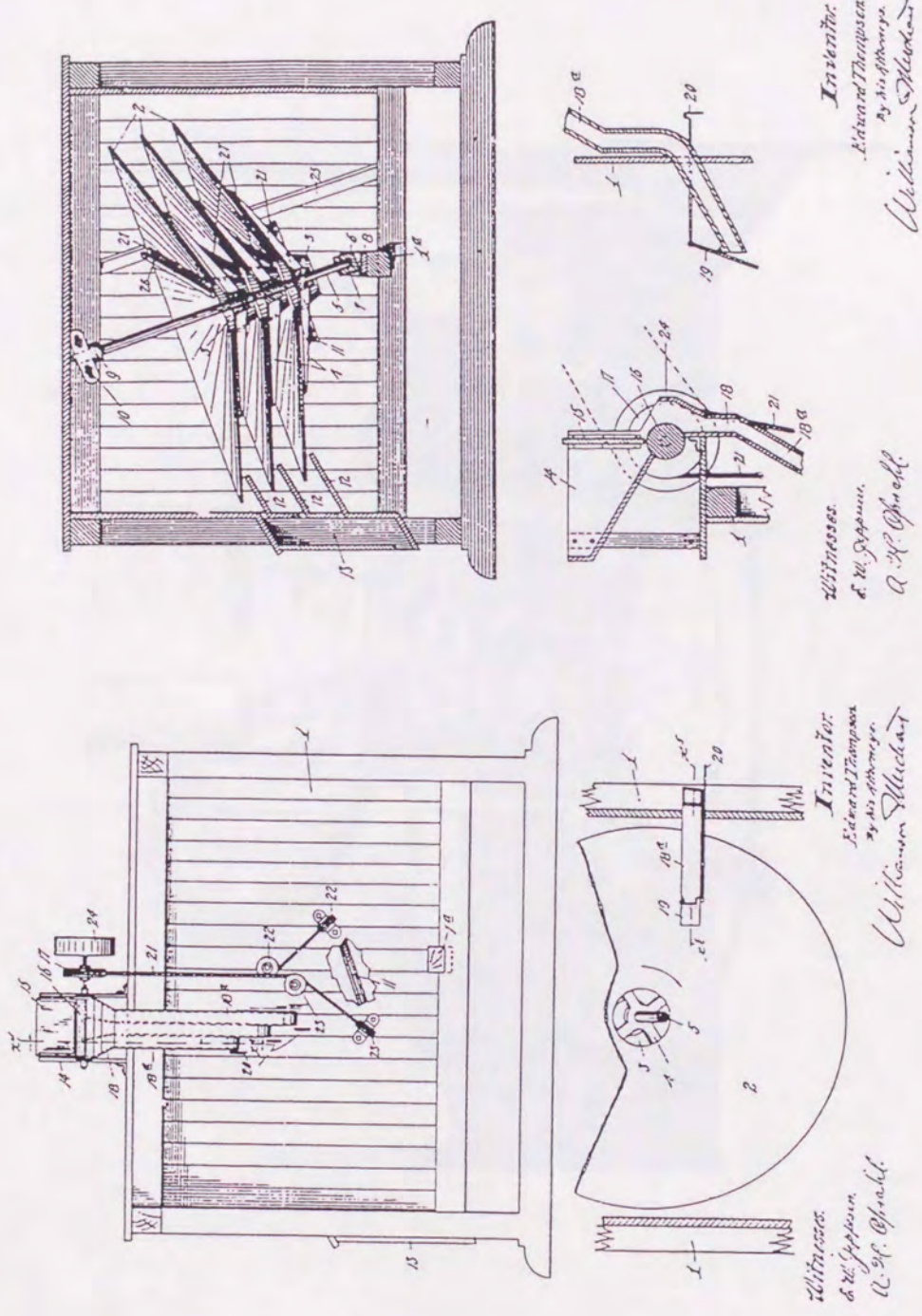


Fig. 1.4 Thompson's separator

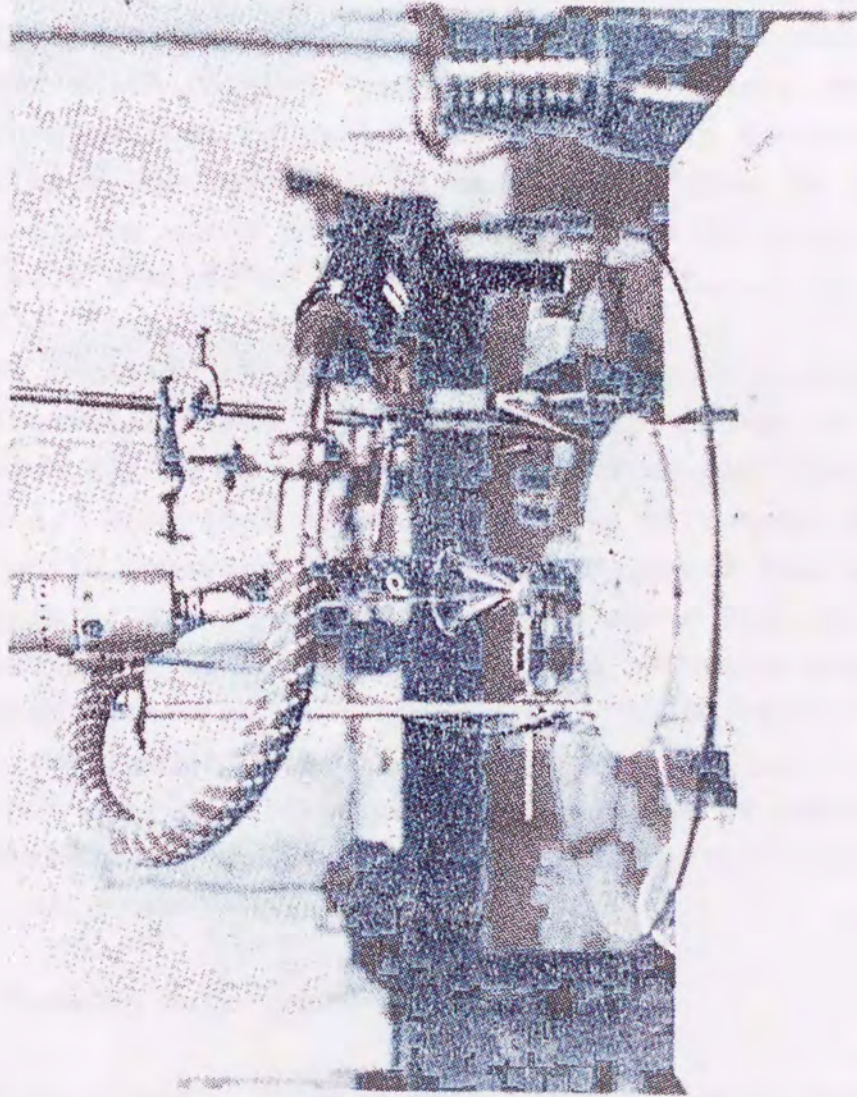


Fig.1.5 Inclined rotating disk method

Sugimoto[23-24] improved this machine with the addition of a scraper for the purpose of unraveling a flock of nonspherical particles on a disk.

By a rotational cone shown in Fig. 1.6, Yamamoto et al.[25-27] reported the advancement of separation accuracy and classification of various particle shapes compared to the inclined rotating disk. Adding vibrated movement to a rotational cone, fine powders could be separated by their shapes.

Furuuchi et al.[28-29] invented a rotating cylinder with a row of blades. As shown in Fig. 1.7, it consisted of a tilted cylinder which rotated very slowly and had many parallel blades. The non-spherical particles were carried up to the cylinder's higher side because each blade shoveled them up, but the spherical particles moved to the lower side by the tilted effect. There were 2 kinds of apparatus, batch type(a) and continuous type(b).

An inclined vibration plate separator was developed by Abe and Hirose[30] (see Fig. 1.8). It was devised as an inclined vibration feeder in which the higher side was the direction of the feed. Spherical shapes moved down by reason of an inclination, while nonspherical shapes moved upward due to vibration. The merit of this method was that it could deal with fine particles because flocks of particles were unraveled with vibration.

When particles were separated by shapes with these instruments, the process was not connected to the particle size, but it could not deal with fine particles because of adhesion. It is considered that the lower limit of the particle size must be 100 to 300 microns.

1.4.3 Passing Rate Type

With gravity, spheres pass through a hole faster than nonspheres. Meloy[31-32] and Endoh[33] proved this fact and suggested the possibility of particle shape separation with sieves.

Hsyng et al.[34] advanced the inclined sieve, as a continuous particle shape separator. A rotating cylindrical sieve as shown in Fig. 1.9, was used by Furuuchi et al.[35], in which particles were collected from an upper-side pan to a lower-side

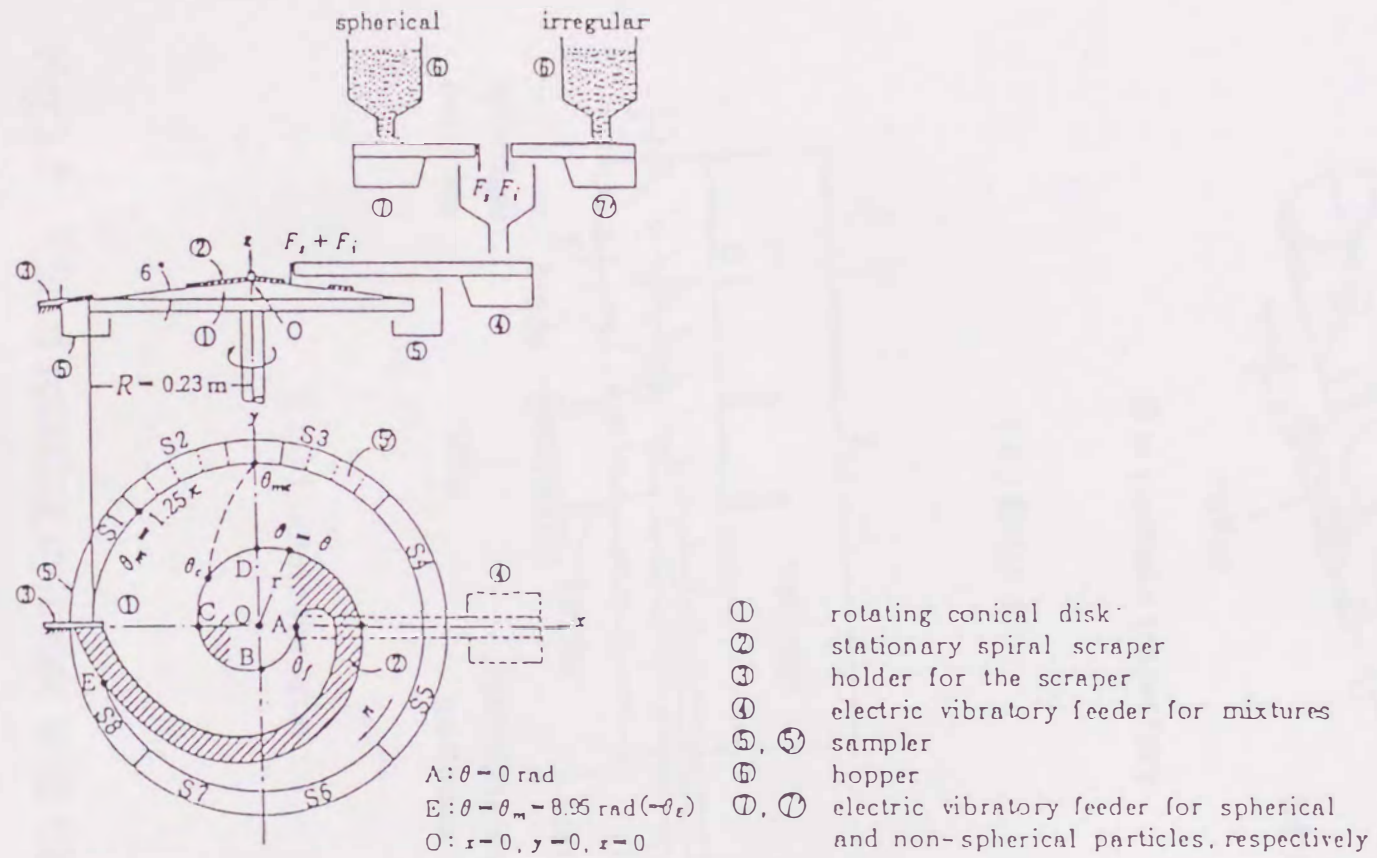
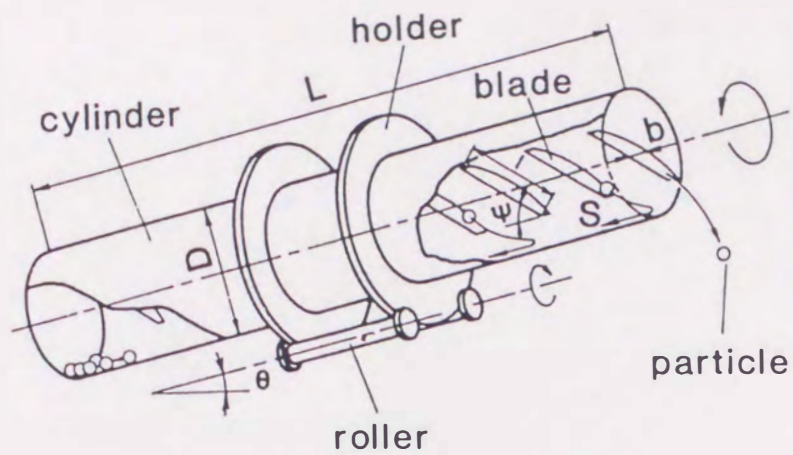
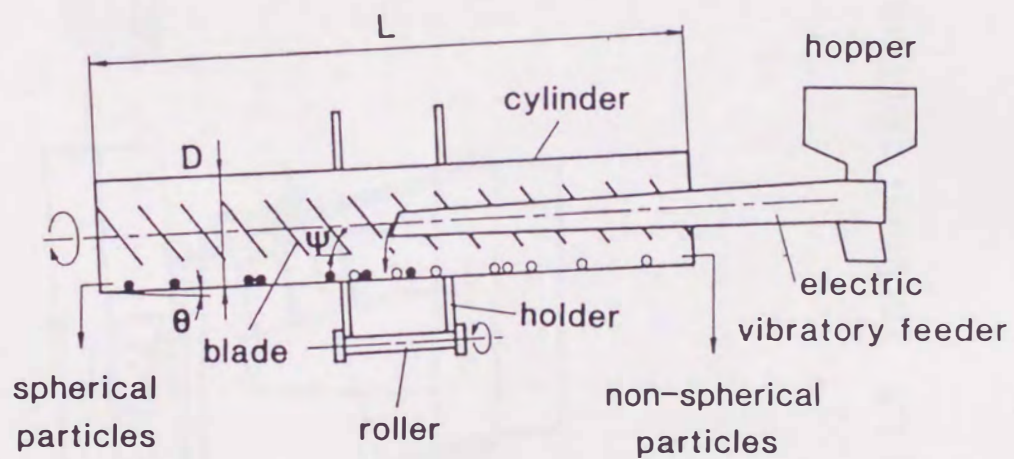


Fig.1.6 Rotating come method



S = particle trajectory

(a) Batch type



(b) Continuous type

Fig.1.7 Tilted rotating cylinder with blades

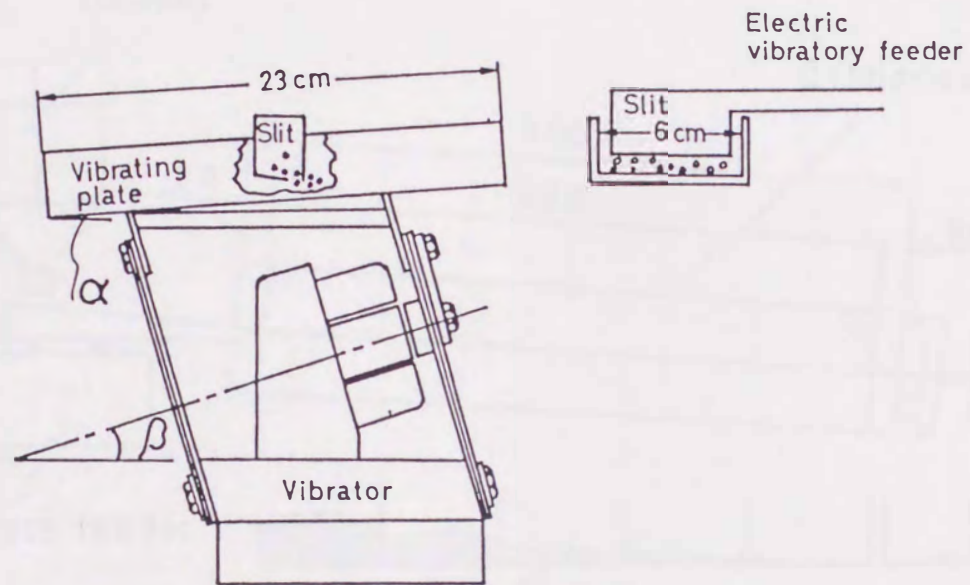


Fig.1.8 Inclined vibration plate

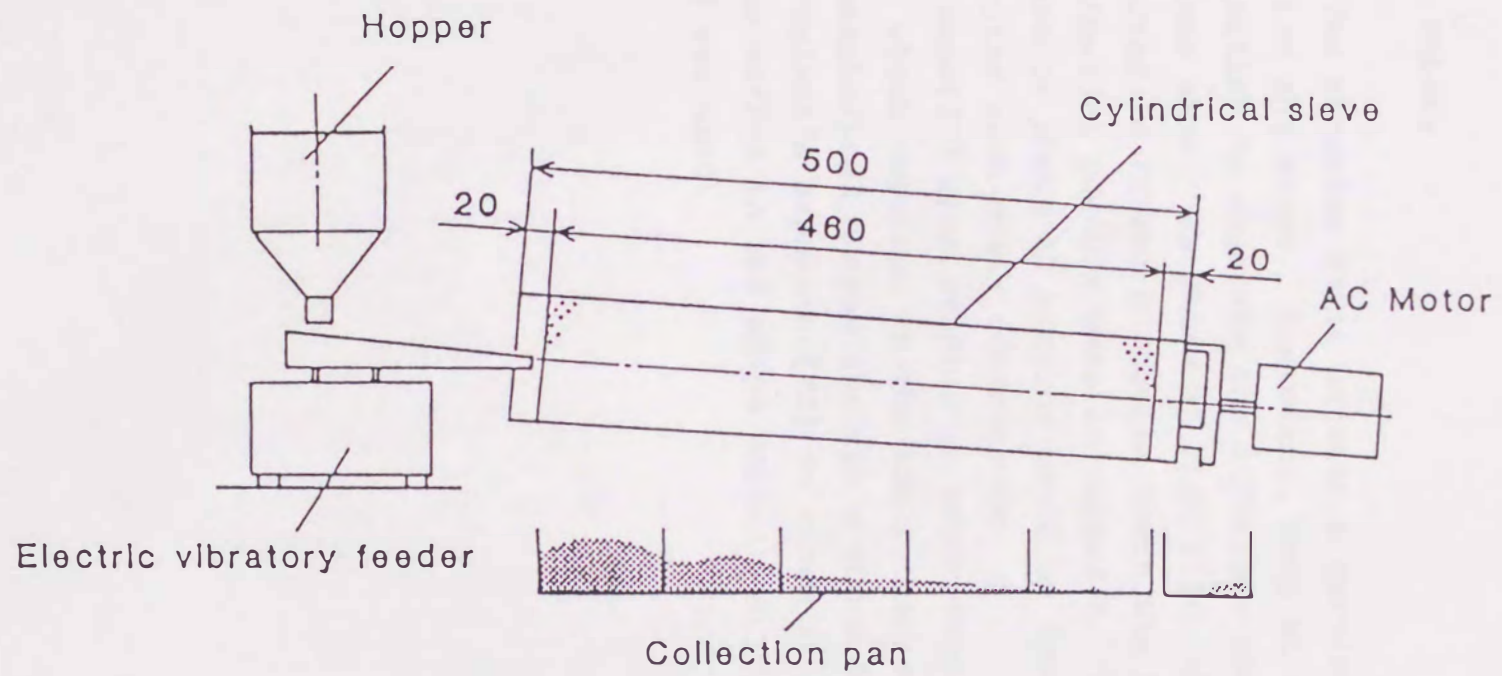


Fig.1.9 Rotating cylindrical sieve method

pan according to spheroidicity. It was reported that needle-like zinc powder was effectively separated by a small blockade.

In passing rate apparatuses, it is easy to distinguish between spherical and rodlike or needle-like particles.

1.4.4 Others

The adhesive force between a particle and a wall depends on its size and shape. Therefore, Sano et al.[36] proposed an adhesion method to separate the different shapes from particles of the same size. As shown in Fig. 1.10, the spherical powders were collected in vessel B because there was strong adhesion, but the nonspherical powders were in vessel A. According to this paper, powders of about 50 microns could be treated, which could not be separated with other instruments.

Sano[37] also studied an adsorption method as shown in Fig. 1.11, which depended on the adsorption selectivity of spherical or nonspherical shapes through a round hole.

Mulari's separator[38] is shown in Fig. 1.12. It is a unique method in the shape separation process, and in this case fluid was used.

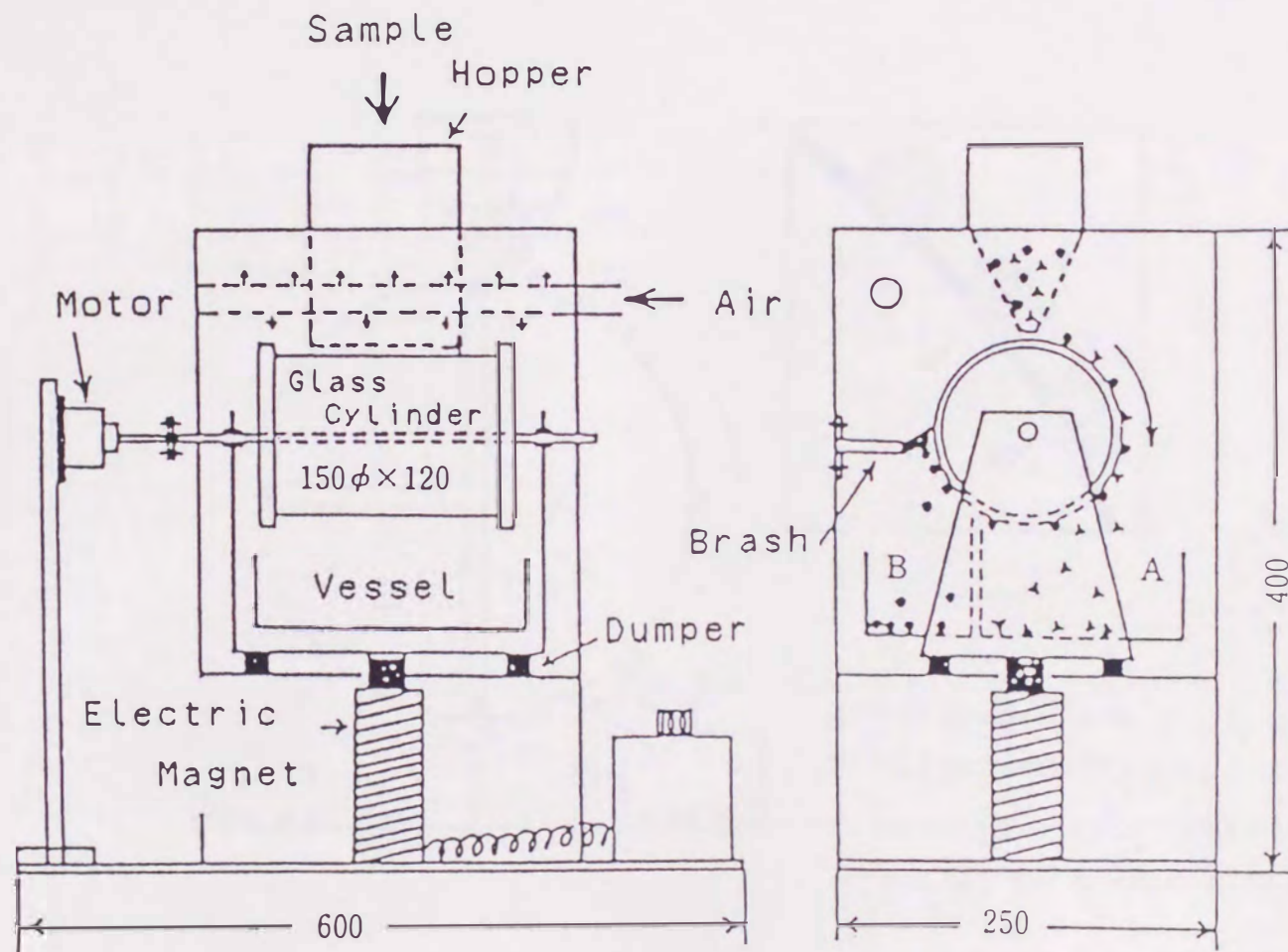


Fig.1.10 Adhesion method

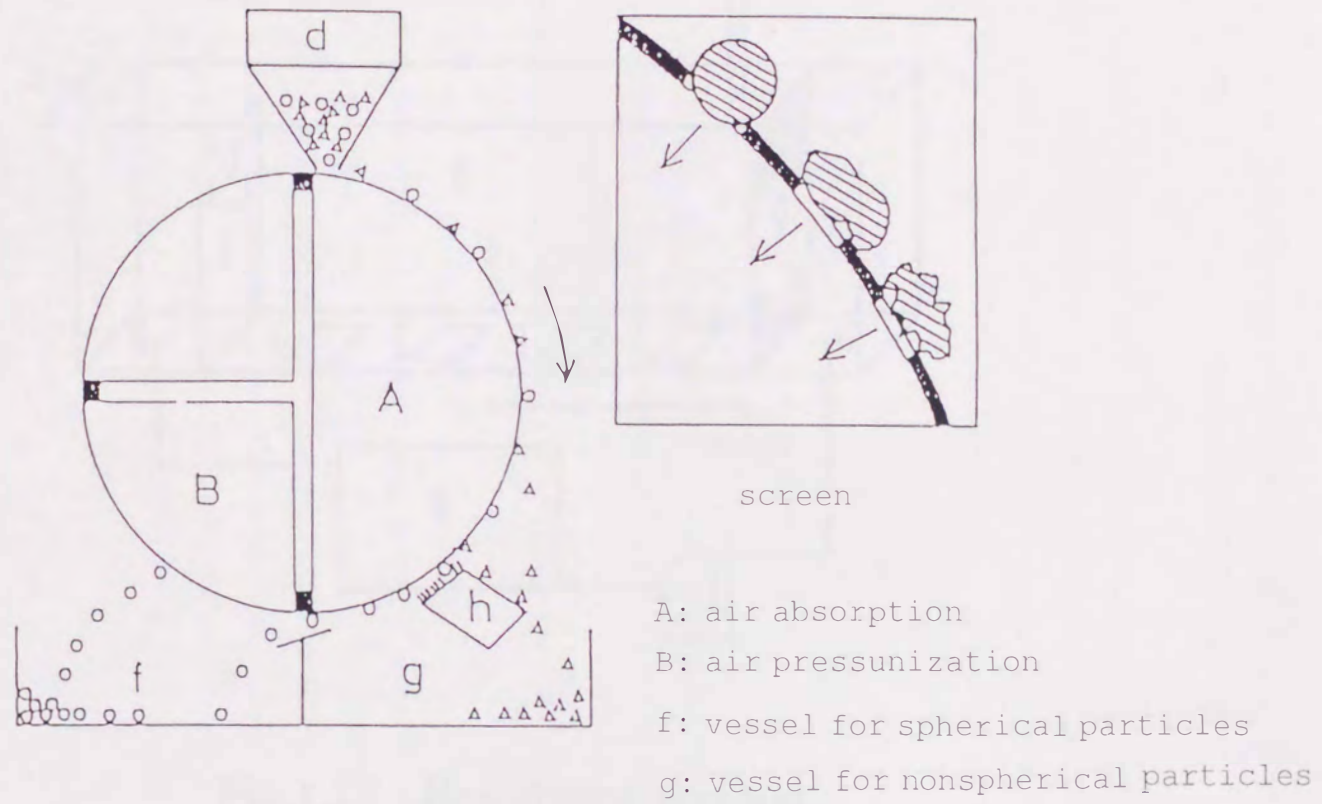


Fig.1.11 Absorption method

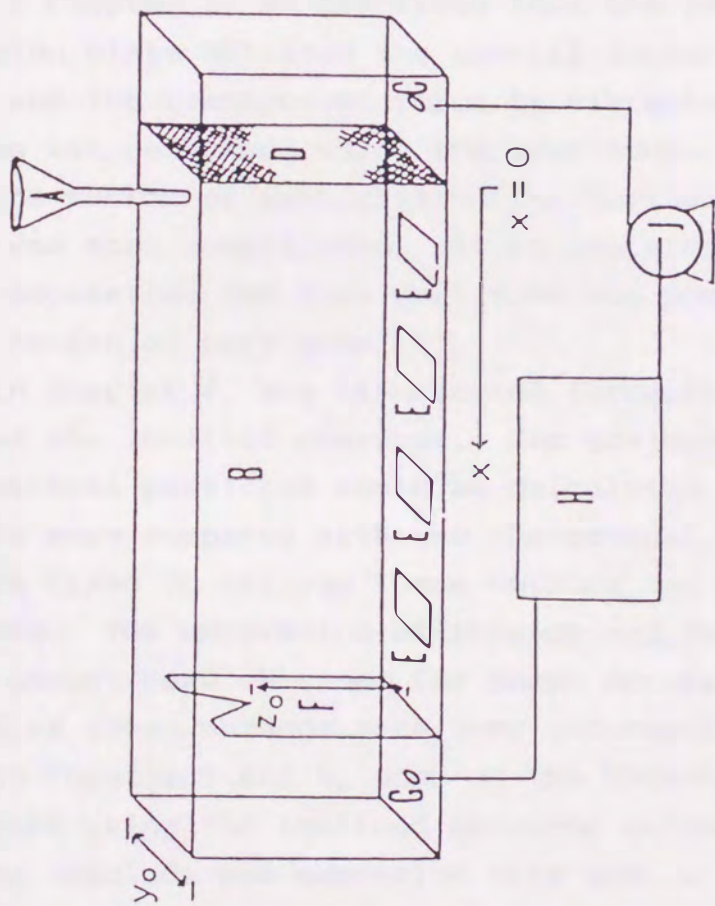


Fig.1.12 Resistance method

1.5 Order of presentation

We developed three types of particle shape separators: an inclined vibration plate, a horizontally circular plate and an inclined conveyor.

These apparatuses belong to the rolling or sliding type and used different trajectories between spherical and nonspherical particles. However, the motion of the particles and the forces working on the particles are different.

In Chapter 2, we described that the particle on the inclined vibration plate obtained the partial force of gravity by inclination, and the transported force by vibration. The accurate shape sorting was performed using the apparatus.

The motion of particles on the horizontally circular motion plate was more complicated. It is explained in Chapter 3. The shape separation for fine particles was possible because of the rapid motion of particles.

In Chapter 4, the transported force is worked by the moving belt of the inclined conveyor. The trajectories of spherical and nonspherical particles could be calculated. The experimental results were compared with the theoretical trajectories.

We tried to analyze these motions and studied the experimental data. The separation efficiency and the limit of the processed amount were obtained for these apparatuses. The characteristics of these methods were very interesting individually.

In Chapter 5 and 6, some of the industrial applications were presented using the inclined conveyor method.

We conclude and summarize this thesis in Chapter 7.

Chapter 2. INCLINED VIBRATION PLATE

2.1 Introduction

An inclined vibration plate was the first method developed by our group for particle shape separator. Abe et al.[30] studied shape separation using vibration; however, the direction of inclination was parallel to the movement of the particles. We improved the direction to the perpendicular to the long axis for avoiding the interruption of spherical and nonspherical particles. The apparatus shown in Fig. 2.1 has a simple structure, just as an inclined vibrating feeder with a wide trough.

The other characteristic of this method is an accurate shape separation. A very high efficiency was obtained by this method. It would be possible to use this apparatus not only for a separator but also for a shape analyzer.

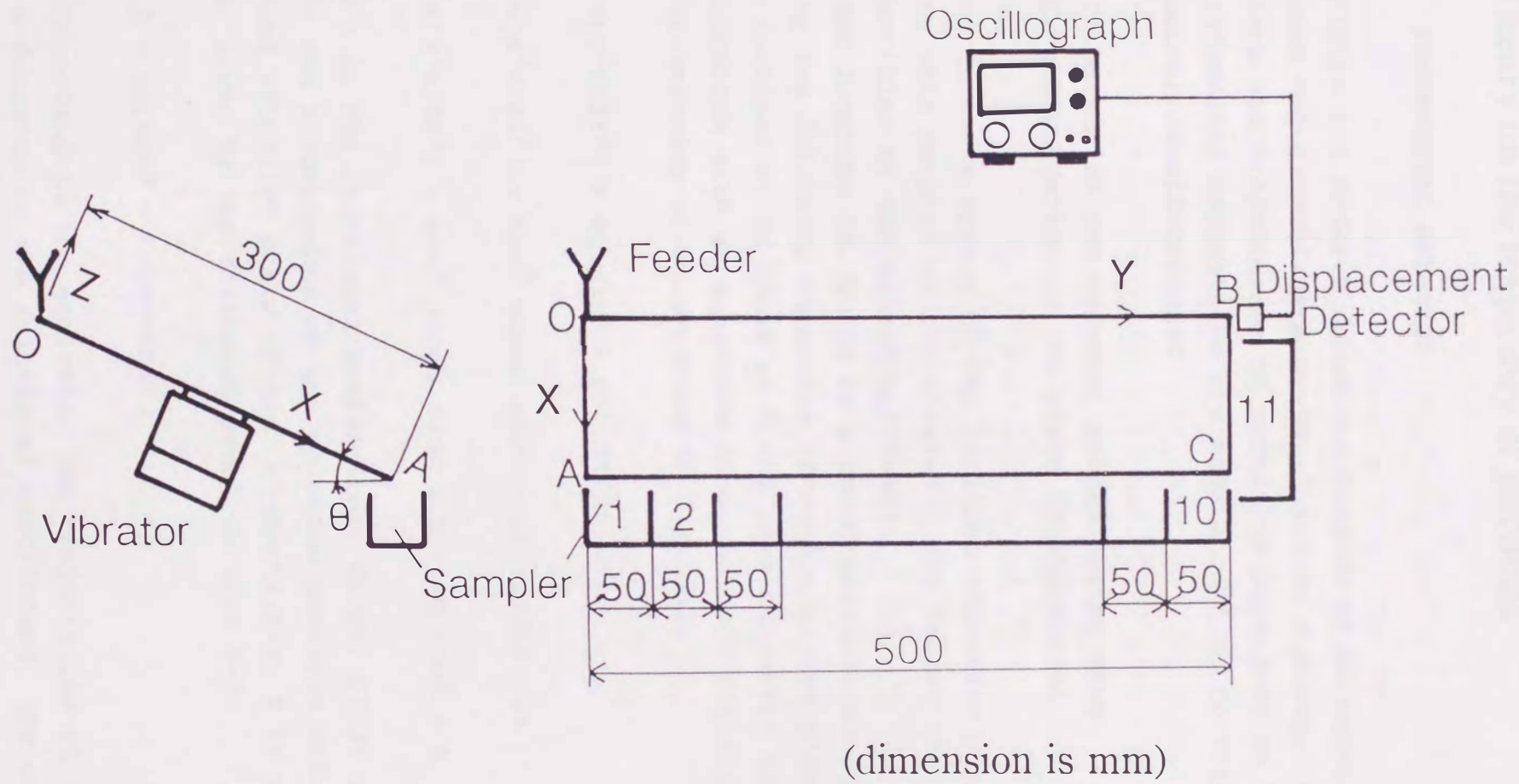


Fig.2.1 Inclined vibration plate

2.2 Theory on the trajectory of particles

2.2.1 FUNDAMENTAL RELATION

Figure 2.1 shows a schematic diagram of an experimental apparatus and a coordinate system fixed on a plate. We tried to calculate the trajectories of particles dependent on the shape. The fundamental assumptions are made according to the following fundamental considerations:

1. particles are material points having mass
2. the vibration of the plate is sinusoidal

The coordination system of the inclined vibration plate considered in this chapter is illustrated. The forces are acting on the particles by the vibration[39-40].

The location (X, Y, Z) of a point particle could be given by solving the following equations of motion on the plate, when the plate inclined at an angle of θ and was subjected to a sinusoidal vibration with an amplitude of c , a throw angle of α and an angular velocity of ω , as shown in Fig. 2.1:

$$m(d^2X/dt^2) = mg \sin\theta - \mu N((dX/dt)/u) \quad (2-1)$$

$$m(d^2Y/dt^2) = ma\omega^2 \sin\omega t \cos\alpha - \mu N((dY/dt)/u) \quad (2-2)$$

$$m(d^2Z/dt^2) = ma\omega^2 \sin\omega t \sin\alpha + N - mg \cos\theta = 0 \quad (2-3)$$

where μ is the frictional coefficient; dX/dt , dY/dt and dZ/dt the X-, Y- and Z-components of the relative particle velocity to the inclined vibration plate origin, respectively. R is a reaction force, given by the following equation from $Z=0$:

$$N = mg(\cos\theta - K\sin\alpha\sin\omega t) \quad (2-4)$$

According to the analysis, the trajectories of the particles were a function of the frictional coefficient, the vibration

intensity and an inclination angle.

2.2.2 TRAJECTORY OF PARTICLES

The trajectories of particles[41] were calculated for several frictional coefficients as shown in Fig. 2.2. For the lower vibration intensity, the trajectories were dependent on friction, and the particles could be sorted due to the friction. For the higher vibration intensities and higher inclinations, the variation in the trajectories becomes smaller. The experimental results qualitatively agreed with the calculated trajectories.

The transport velocity of particles by vibration was also dependent on the friction. Figure 2.3 shows the average transport velocity of a silica sand determined from the measurements for a hundred particles at $\theta=0$, and the calculated values are drawn.

The kinetic friction of silica sand used in this experiment was considered to be 0.5 to 0.7 from the results. On the other hand, the friction of glass bead was considered to be about 0.01 by Abe. Therefore, silica sand can be separated from glass bead by the inclined vibration plate, and the behaviors could be estimated by the model analysis previously carried out.

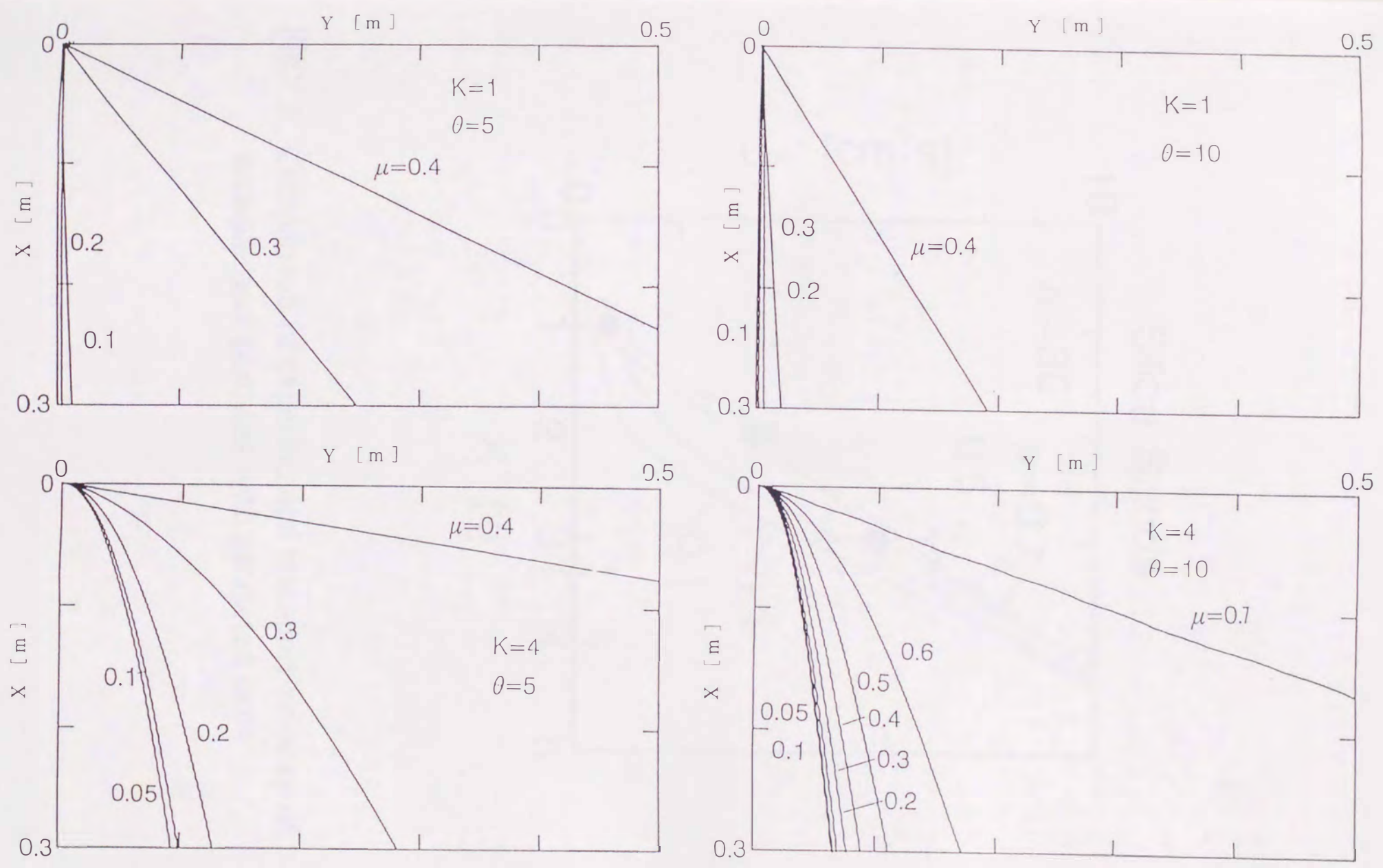


Fig.2.2 Trajectory of frictional particles

2.2 Accuracy of prediction of glass beads and sand

2.2.1 Accuracy of prediction

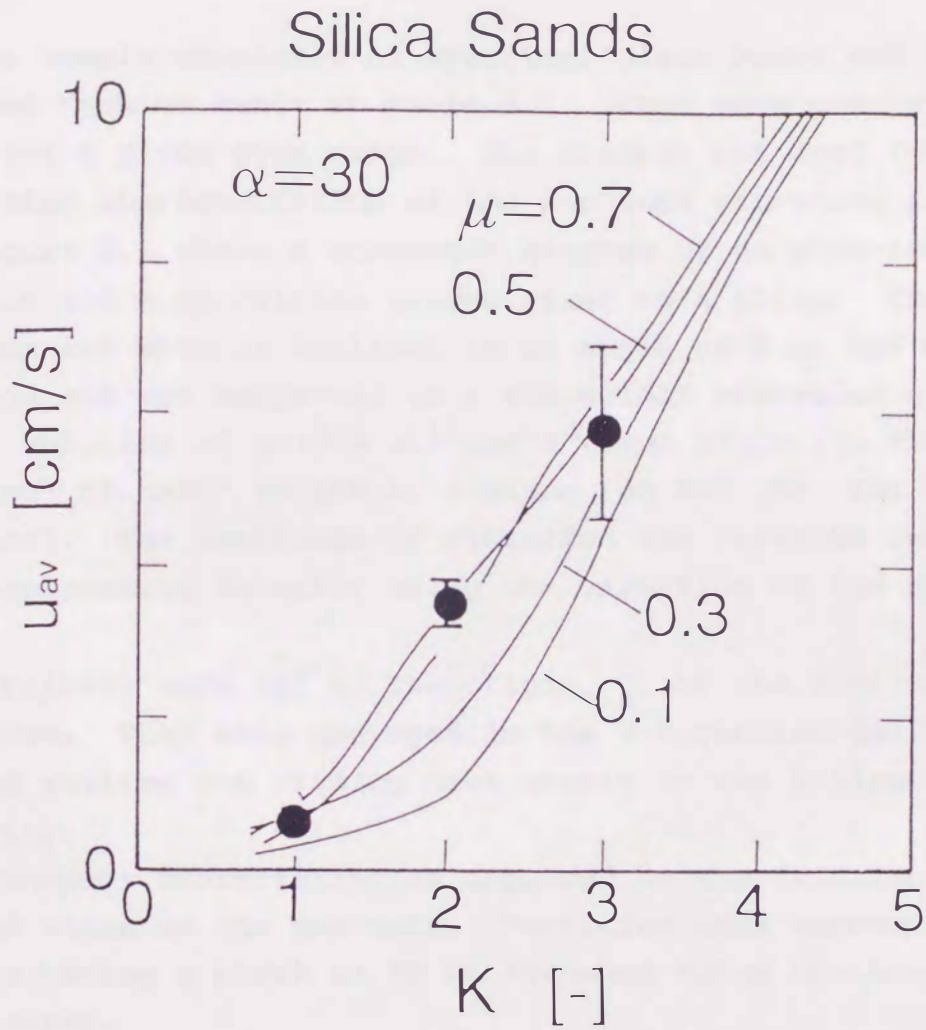


Fig.2.3 Comparison of experimental transport velocity of nonspherical particles with predicted ones

2.3 Accurate shape sorting of glass beads and sands

2.3.1 MATERIAL AND EXPERIMENT

The sample consisted of spherical glass beads and irregularly shaped Kashima sands in Table 2.1. They were previously sieved for a given size range. The mixture was used for testing the sorting characteristics of the inclined vibration plate.

Figure 2.1 shows a schematic diagram of an experimental apparatus and a coordinate system fixed on a plate. The aluminum plate was set with on inclined at an angle of θ in the horizontal direction and was subjected to a sinusoidal vibration with an angular velocity of $\omega=100\pi \text{ s}^{-1}$ and a throw angle (in the Y-direction) of $\alpha=30^\circ$ to the X, Y-plane (at $\theta=0$, in the horizontal direction). The amplitude of vibration was variable and measured by a displacement detector using the variation of the eddy current.

Particles were fed to the origin, 0, of the inclined vibration plate. They were conveyed in the Y-direction due to vibration and rolling and sliding down nearly in the X-direction due to gravity.

Transport characteristics depended on the frictional properties and shape of the particle. Particles were recovered by samplers having a width of 50 mm attached below the bottom edge of the plate.

The samplers were numbered from 1 to 11 from the origin, 0, along the Y-direction. Spherical or nonspherical particles recovered in the sampler were weighed after hand sorting. The separation efficiency could be calculated.

Experimental conditions are shown in Table 2.1.

2.3.2 SEPARATION PERFORMANCE[42]

Figure 2.4 shows the effect of nonspherical particles regarding the separation characteristics of an inclined vibration plate. The recovery distributions of the spherical (glass bead)

Table 2.1 Materials and experimental conditions

sample		
materials	spherical glass bead	nonspherical Kashima sand
size range [mm]	0.5~0.71	0.5~0.85
mixing ratio	1	: 1
experimental conditions		
frequency f [Hz]	50	
amplitude a [mm]	0.063~0.24	
throw angle α [degree]	30	
inclination θ [degree]	5, 10, 15	

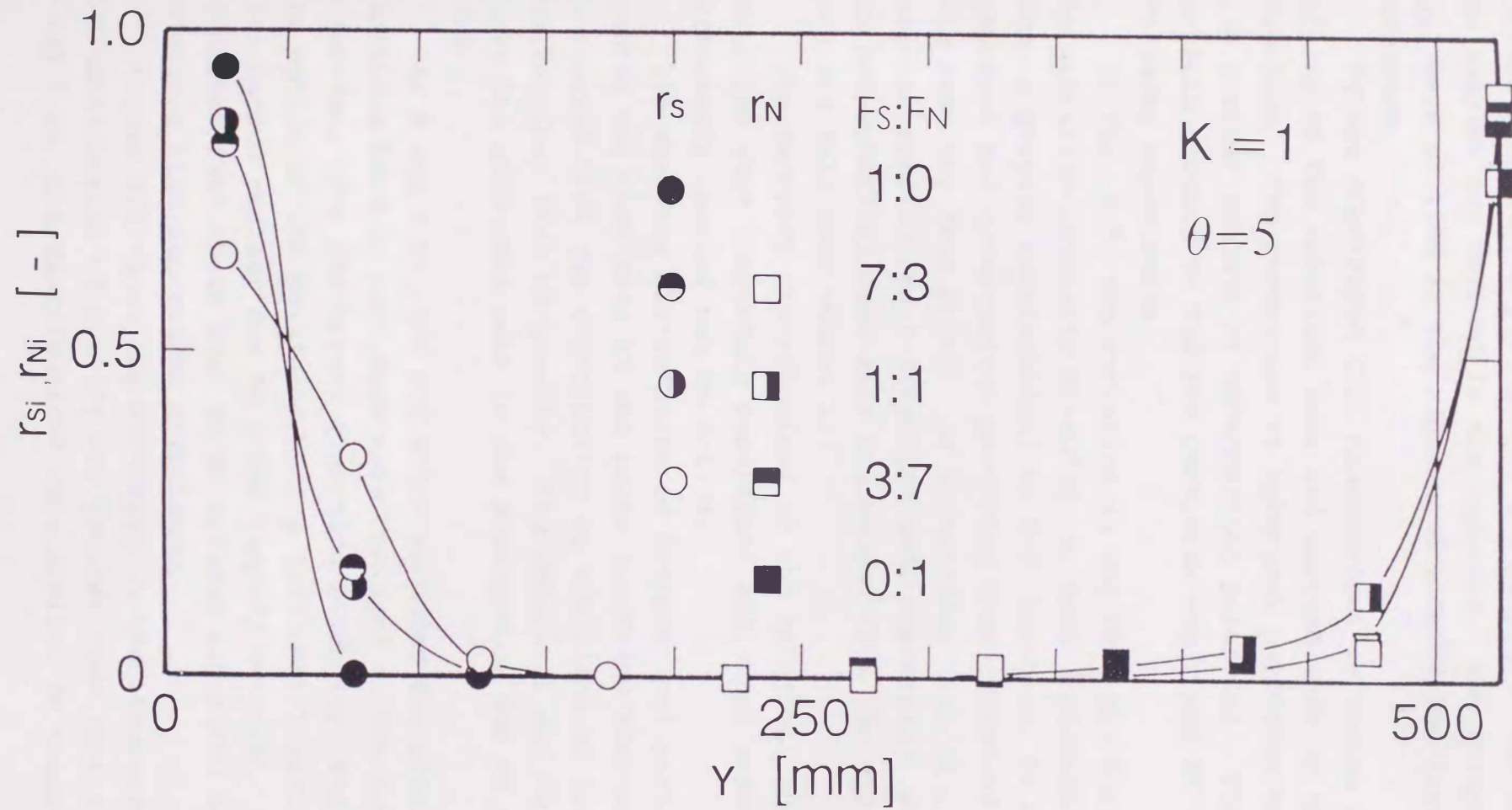


Fig.2.4 Recovery of spherical and nonspherical particles in the inclined vibration plate

and nonspherical particles (Kashima sand), r_{Si} and r_{Ni} , were plotted against the position of the sampler. The recoveries in the sampler are defined in the Appendix. The values of r_{S11} and r_{N11} were plotted in the right hand side of the figure as a reference.

It was considered that nonspherical particles obstructed the rolling of the spherical ones and carried them in the transport direction. The recoveries of spherical particles became lower with greater amounts of nonspherical particles. The nonspherical particle content in the fed particles was fixed at 50% in the following experiments.

In Fig. 2.5, the variation in the recovery distribution with the vibration intensity $K(=a\omega^2/g, a$; half-amplitude of vibration, g gravity acceleration) at $\theta=5^\circ$ is shown. At $K=0.67$, both spherical and nonspherical particles were collected in the vessels near the feed point. As K increased ($K=1.34$), particles were conveyed in the Y-direction and, especially, almost all of the non-spherical ones were discharged from the end of the plate (BC) and fell into vessel 11.

The recovery distributions of the spherical and nonspherical particles were completely separated, and shape separation was efficiently carried out at $K=1.34$.

The recovery distribution of nonspherical particles shifted towards the feed side at the lower vibration intensity. It was considered that the contribution of vibration to conveying was smaller than that of gravity. The spherical and nonspherical particles slid down near in the X-direction due to the inclination.

As K was 2.01, the vibration exceeded the gravity. The particles hard to roll down were conveyed in the horizontal direction. For the higher vibration intensity, the difference in the motion of the particles having different frictional properties became smaller due to their jumping motions. The results indicated that there must be an optimum vibration condition for obtaining high-separation efficiency.

Figure 2.6 shows the variation in the recoveries at $\theta=10^\circ$. The contribution of gravity was greater than that at $\theta=5^\circ$. When K was 0.68, the distributions were similar to those at $\theta=5^\circ$.

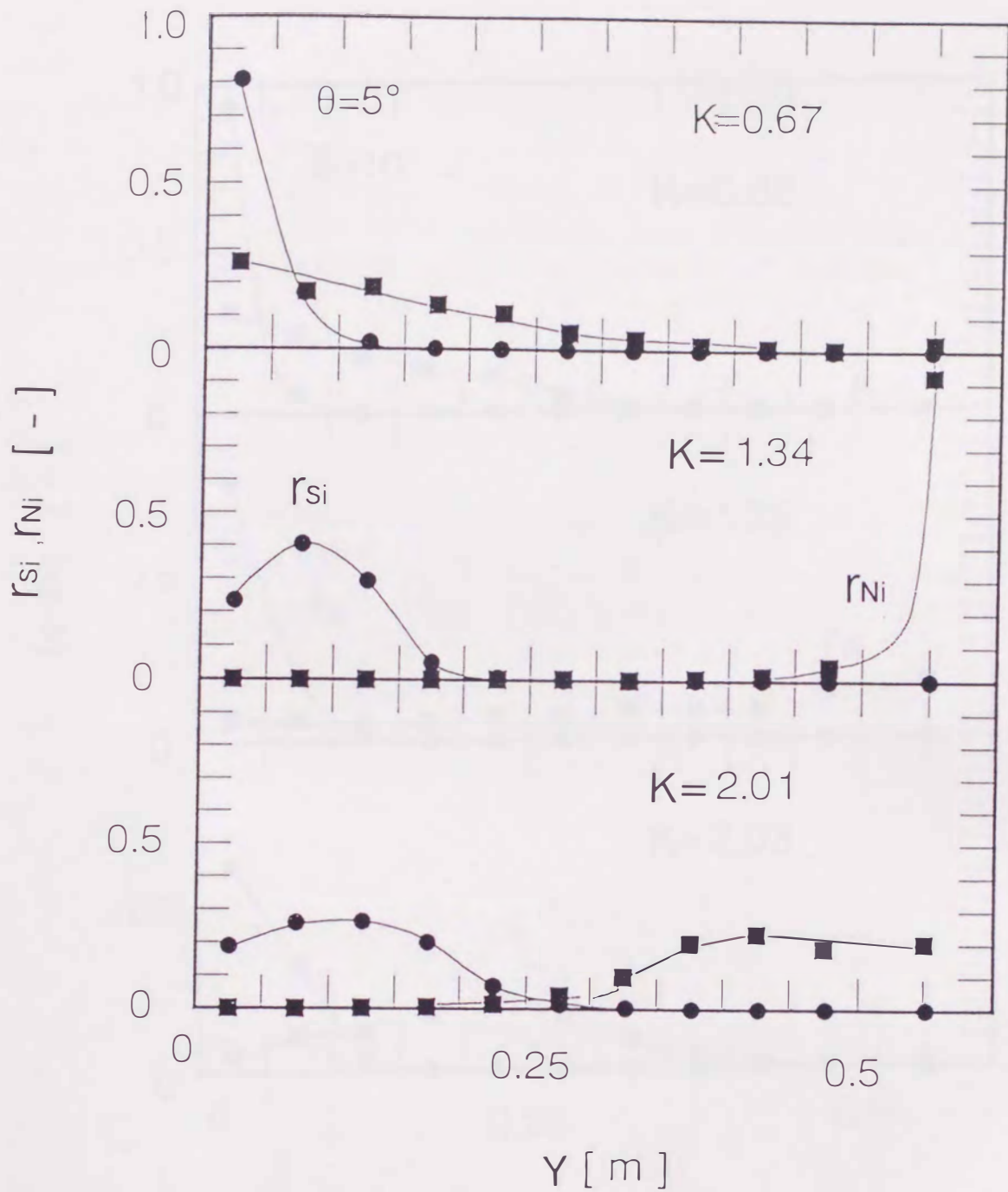


Fig.2.5 Recovery of spherical and nonspherical particles affected by the vibration intensity , $\theta = 5^\circ$

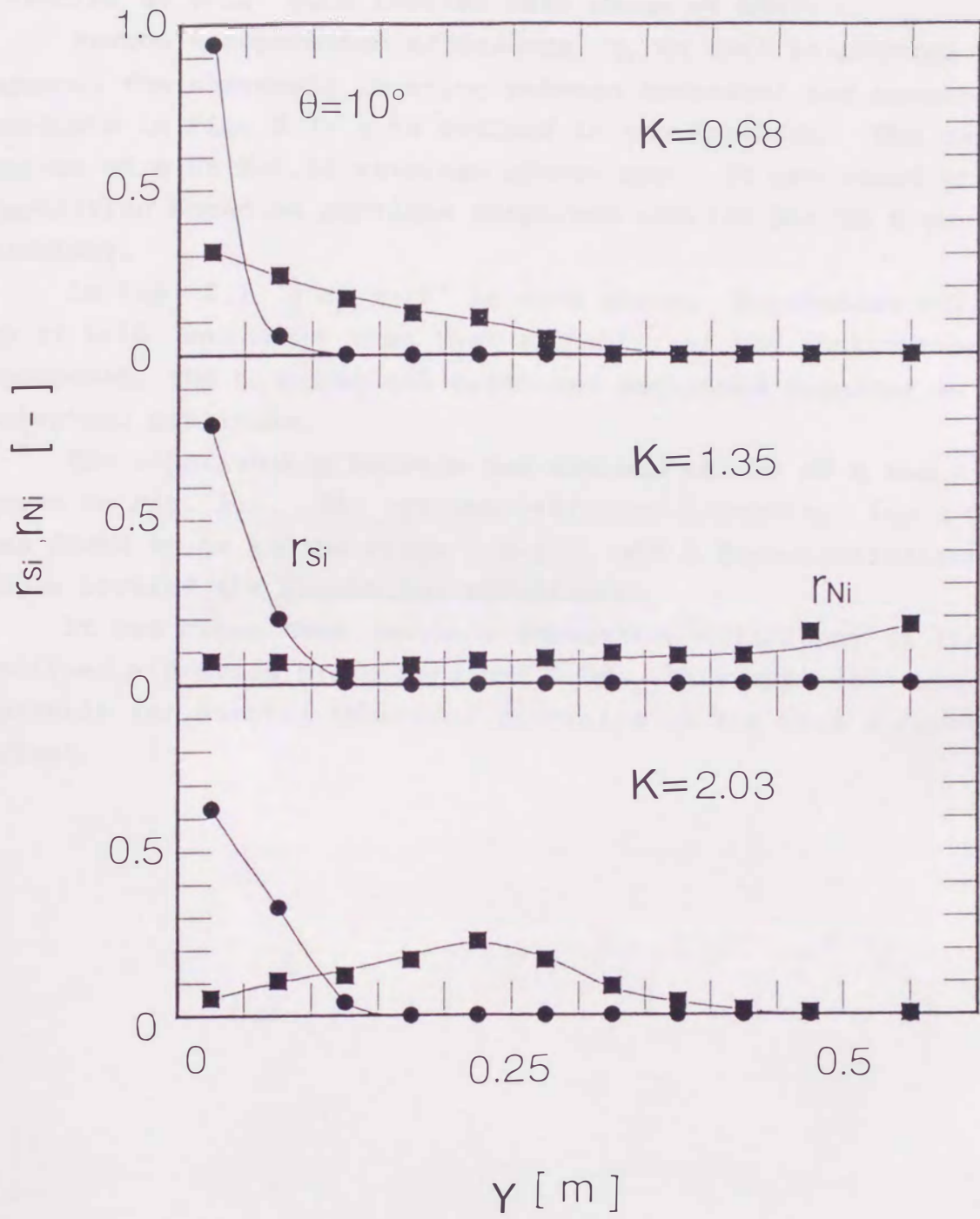


Fig.2.6 (same as Fig.2.5), $\theta = 10^\circ$

However, nonspherical particles were widely dispersed on the plate for the higher vibration intensity. The separation efficiencies at $\theta=10^\circ$ were lowered than those at $\theta=5^\circ$.

Newton's separation efficiency, η , at $\theta=5^\circ$ is plotted against the threshold location between spherical and nonspherical products in Fig. 2.7; η is defined in the Appendix. The maximum values of η at $K=1.34$ attained almost one. It was found that separation based on particle shape was carried out to a very high accuracy.

In Fig. 2.7, η at $\theta=10^\circ$ is also shown. Separation efficiency at $\theta=10^\circ$ was lower than that at $\theta=5^\circ$. As the inclination increased, the nonspherical particles decreased together with the spherical particles.

The relationship between the maximum values of η and K is shown in Fig. 2.8. The optimum vibration intensity for $\alpha=30^\circ$ was found to be in the range 1.3-1.4, and a high-inclination angle lowered the separation efficiency.

It was clear that Newton's separation efficiency of the inclined vibration plate attained 0.99. This apparatus was suitable for sorting spherical particles to the most accurate extent.

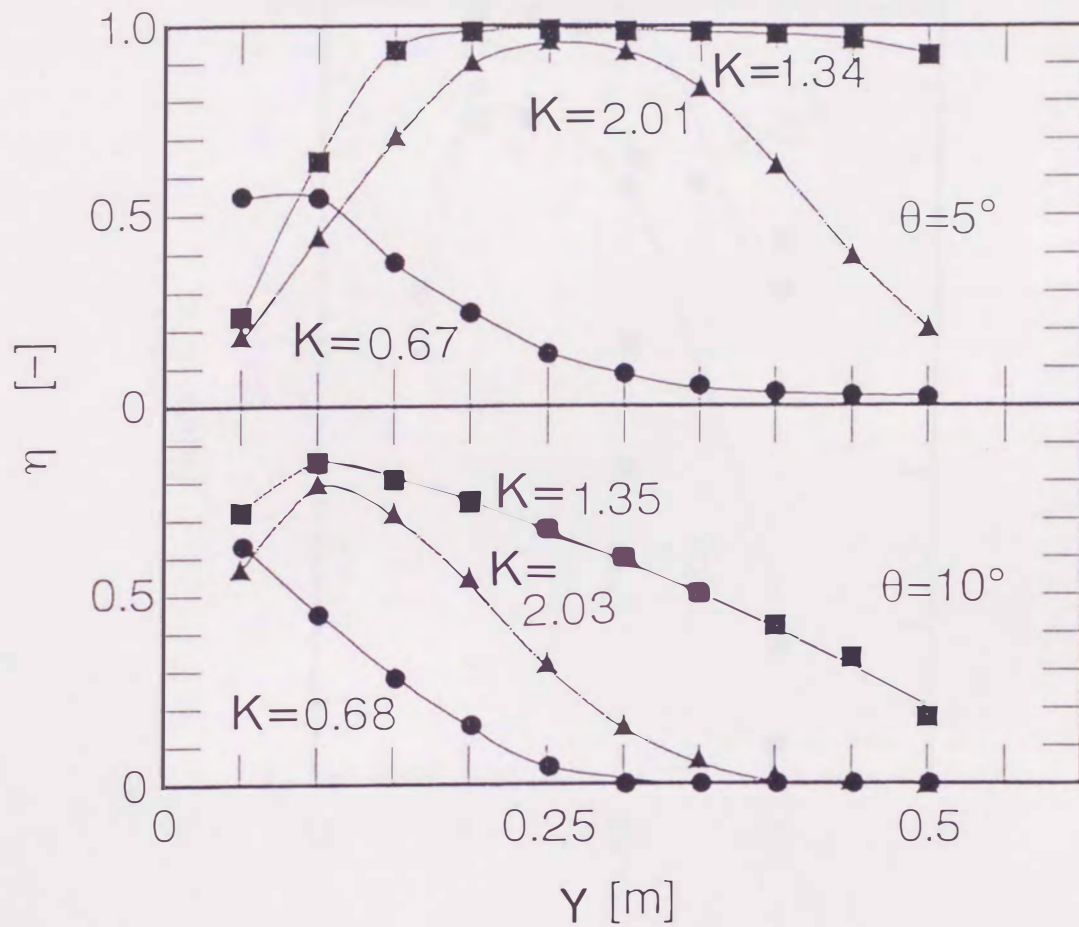


Fig.2.7 Newton's separation efficiency affected by the vibration intensity and the inclination angle

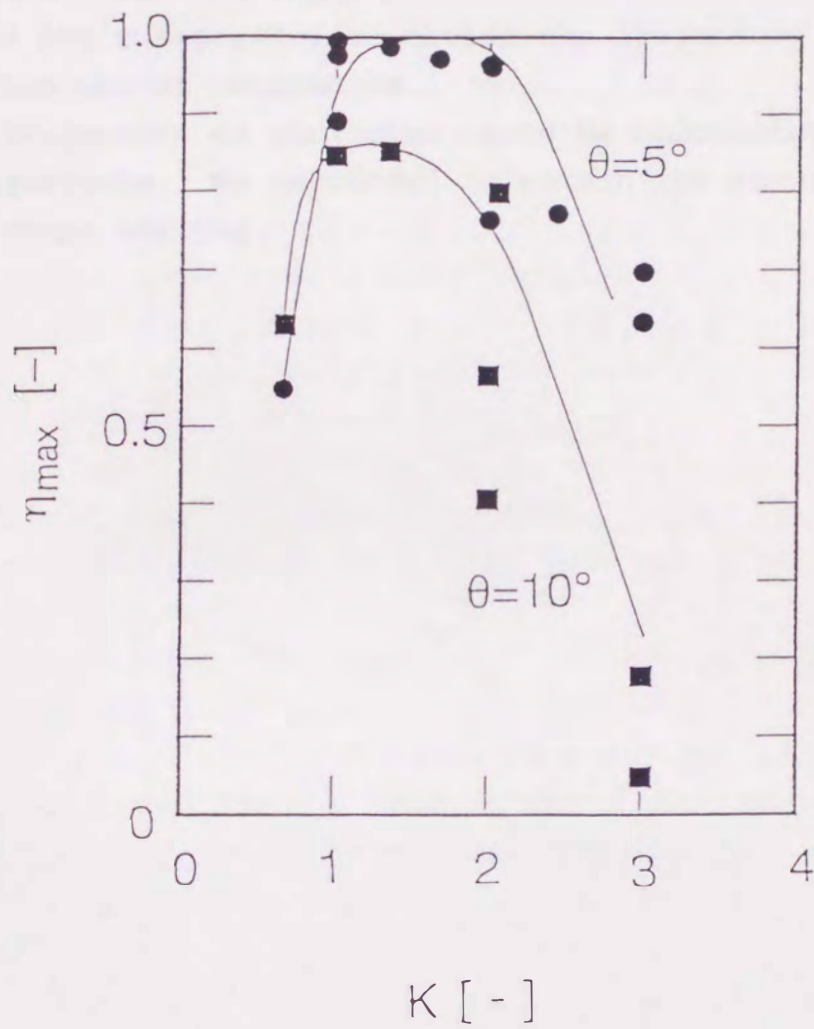


Fig.2.8 Effect of intensity of vibration on maximal Newton's separation efficiency of an inclined vibration plate

2.4 Conclusions

This chapter discusses the separation performance using the inclined vibration plate. It is very simple in structure and requires low cost. We improved the inclination direction compared with Abe's separator to divide the trajectory of the spheres from one of nonspheres.

The trajectory of particles could be calculated by the kinetic equations. We succeeded to obtain the result of the accurate shape sorting.

Chapter 3. HORIZONTALLY CIRCULAR MOTION PLATE

3.1 Introduction

In the category of the rolling or sliding type, a horizontally circular motion plate was introduced for a second particle shape separator.

The motion of particles on an infinite plate, which had circular motion, has been studied by Zukowski and Scott[43-44]. The result was very useful to sieve particles efficiently, because the relative motion of particles compared with the sieve plate are necessary for effective sieving.

We used the circular plate fixed on the shaking table of a gyratory screen for the separation. The motion beside the circular wall had to be analyzed, and the efficiency of separation was determined.

In this chapter, the separation of particles by shape has been carried out using a newly developed device driven by a horizontally circular motion which is entirely different from the apparatus of the inclined vibration plate. We succeeded in separating not only spherical particles, but also non spherical particles which have dull edges from sharper edged nonspherical particles.

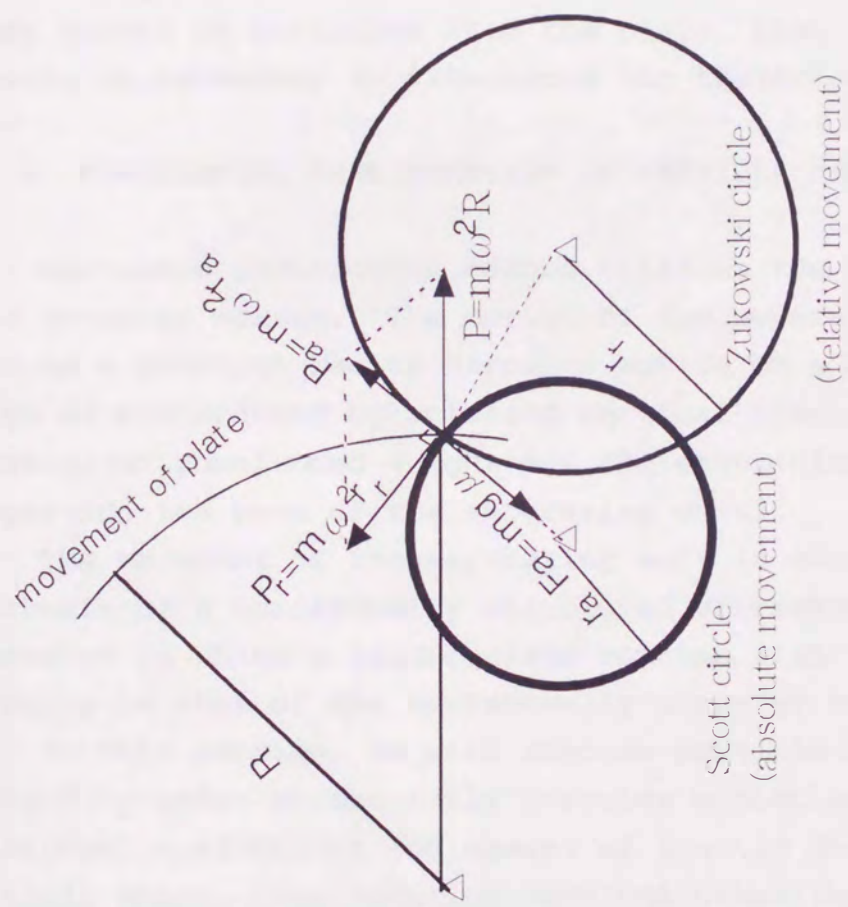


Fig. 3.1 Movement of a particle on the plate

3.2 Analysis of the particle movement

3.2.1 MOTION OF PARTICLE ON HORIZONTALLY CIRCULAR MOTION PLATE

The motion of particles on the plate whose movement was horizontally circular motion was studied with gyro sifter sieving because of the effective operation.

The Zukowski circle as a relative motion and the Scott circle as an absolute motion were calculated using the forces which worked on particles from the plate. (see Fig. 3.1) Kinetic formula is necessary to illustrate the trajectory.

3.2.2 FUNDAMENTAL CONSIDERATION OF PARTICLE BEHAVIOR[45-46]

Our shape distinction method utilizes the motion generator of a gyratory screen. The motion of the separator is characterized as a constant radius circular motion on a horizontal plane which is accompanied by rotating vertical vibration caused by the rotation of unbalanced weight and the elasticity of the springs supporting the base of the separating unit.

The movement of the separating unit is considered to be the synthesis of a horizontally circulated vibration and a vertical vibration in which a tilted plate rotates with the same angular velocity as that of the horizontally circular motion.

In this section, we will discuss particle behavior on a flat plate only under horizontally circular motion with regard to the frictional coefficient and moment of inertia depending upon the particle shape. The rotating vertical vibration was neglected.

The motion of single particle is considered as follows: Let a plate be circularly moving and outlining a circle with the radius, R . For the purpose of explanation, one fixes a reference point in the plate as the origin of a two-dimensional coordinate system.

Although the particle may rotate, it is supposed at first to be a point material with mass m whose motion is influenced by neither aerodynamic effects nor cohesion with the plate.

With the direction of the circulated vibration, being counter-clockwise, the displacement, velocity and acceleration of the reference point of the plate are expressed as follows, respectively, where R and ω are the radius and angular velocity of circular motion :

$$X_t = -R + R \cos\omega t \quad Y_t = R \sin\omega t \quad (3-1)$$

$$dX_t/dt = -R\omega \sin\omega t \quad dY_t/dt = R\omega \cos\omega t \quad (3-2)$$

$$d^2X_t/dt^2 = -R\omega^2 \cos\omega t \quad d^2Y_t/dt^2 = -R\omega^2 \sin\omega t \quad (3-3)$$

X_p and Y_p , being components of particle displacement, the relative velocity vector between particle and the plate, dX/dt , is expressed as

$$dX/dt = dX_p/dt - dX_t/dt \quad (3-4)$$

Because the frictional force of the particle having mass m and kinetic frictional coefficient μ with the plate acts opposite to the direction of dX/dt , the equation of motion of the particle is described as

$$m d^2X_p/dt^2 = -\mu mg (dX/dt) / |dX/dt| \quad (3-5)$$

which is decomposed to

$$d^2X_p/dt^2 = -\mu g (dX/dt) / \{(dX/dt)^2 + (dY/dt)^2\}^{1/2} \quad (3-6)$$

$$d^2Y_p/dt^2 = -\mu g (dY/dt) / \{(dX/dt)^2 + (dY/dt)^2\}^{1/2} \quad (3-7)$$

As the apparent displacement of the particle is the relative displacement of the particle with respect to the plate, both components X and Y are calculated by:

$$X = X_p - X_t \quad (3-8)$$

$$Y = Y_p - Y_t \quad (3-9)$$

Figure 3.2 illustrates some examples of numerical calculation carried out using the previous procedure in which the displacement of a mass fed to the origin of the coordinates at time zero without any initial velocity is plotted with the lapse of time till 0.3 s, depending on the frictional coefficient of the mass with the plate.

In the case of the spherical particle, the frictional coefficient could be considered to be zero where the path of the mass can be imagined without difficulties directly from equations (3-6) and (3-7) as a path symmetrical to that described by the plate with the origin as the point of symmetry.

In the presence of a finite frictional coefficient, it is shown that the path of the mass tends to converge to a circle having a radius which decreases from the same radius as the driving motion as the frictional coefficient increases. The convergence time also decreases with increasing frictional coefficient, and the greater is frictional coefficient, the smaller becomes the displacement of the mass.

Figure 3.3 shows the effects of the initial velocity vector on the behavior of the mass under otherwise the same conditions as in the previous case. In any case, the velocity vector is assessed to decrease with time when the frictional force exists, while it remains unchanged in the case without friction.

According to the previous discussion, it is indicated that generally a nonspherical particle is more likely to lose its mobility towards the assigned direction and stagnate shortly in a certain area on the horizontally circular motion plate in comparison with a spherical particle.

3.2.3 ANALYSIS OF PARTICLE BEHAVIOR BESIDE WALL[47]

The particle movement on the infinite plate, which moved with a circular motion, was discussed in the last section, 3.2.2. If a circular wall stood on the plate, particles would be running beside the wall in opposite direction to the circular motion as an experimental result.

This movement was similar to the one of the particles on the

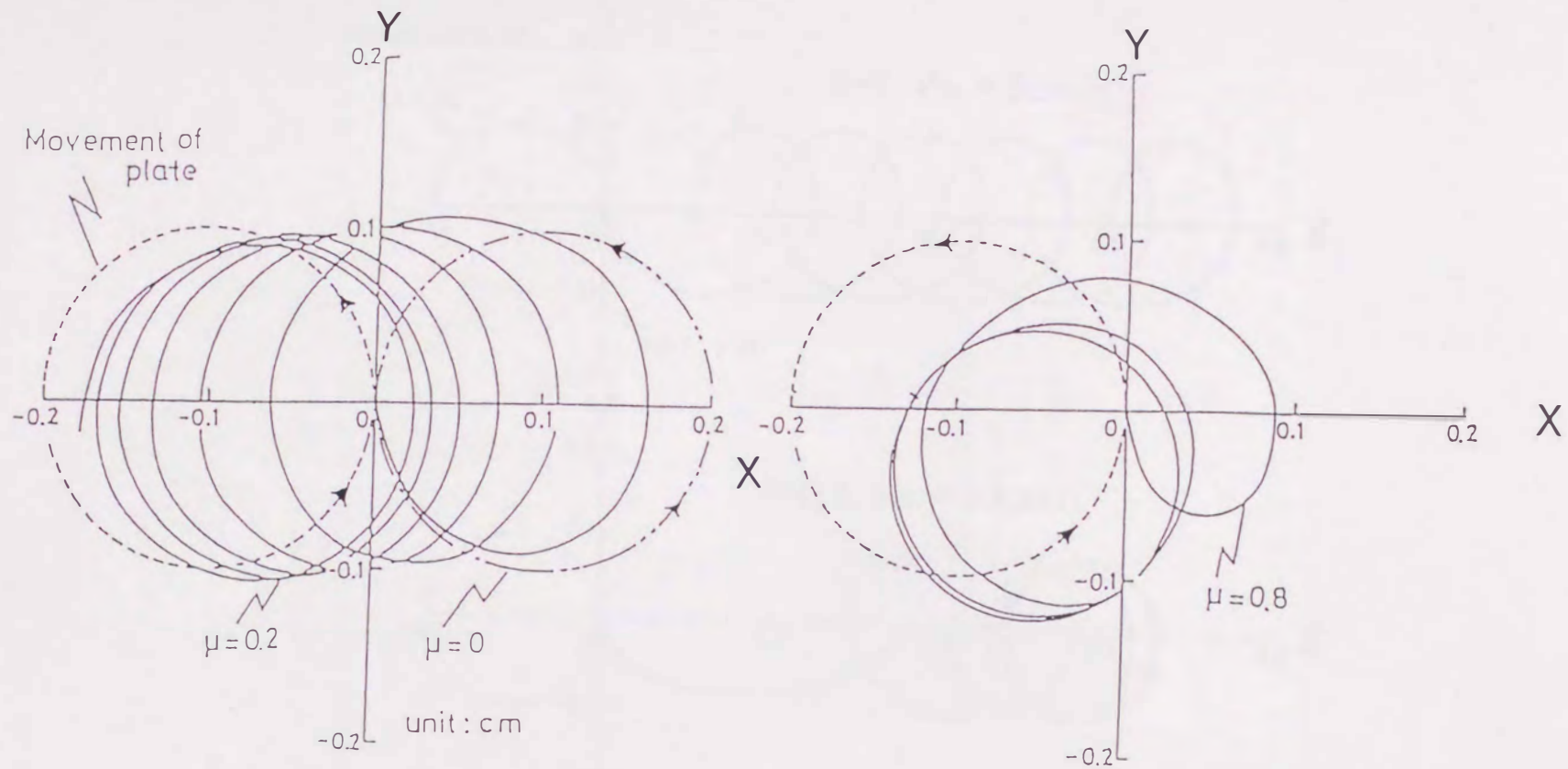


Fig.3.2 The movement of a particle on horizontally circular motion plate

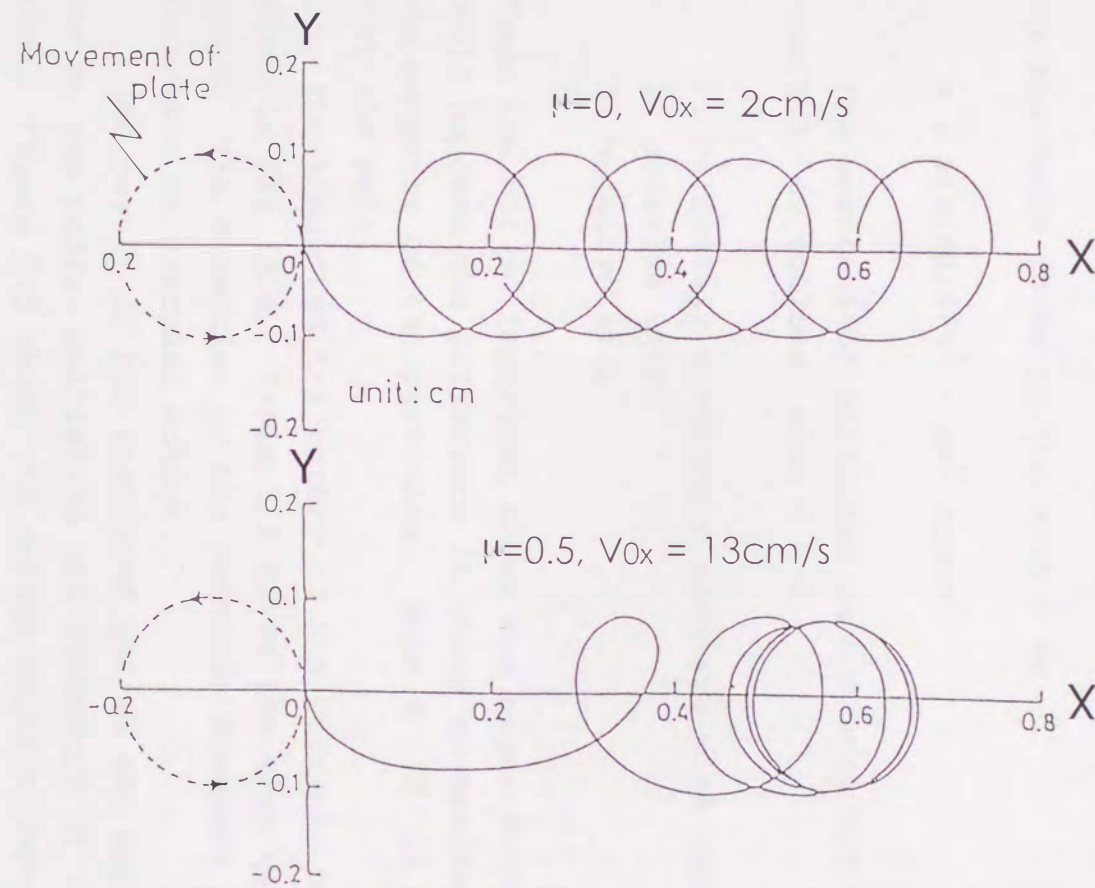


Fig.3.3 The movement of particle with the initial velocity on horizontally circular motion plate

vibration feeder[39-40, 49-52]. The equation of particle movement on the circular motion plate with a circular wall is as follows:

$$m \frac{d^2x}{dt^2} = mR \left(\frac{d\beta}{dt} \right)^2 - N \quad (3-10)$$

$$m \frac{d^2y}{dt^2} = -F_1 - F_2 \quad (3-11)$$

The residence force on the wall N is

$$N = m \left(R \left(\frac{d\beta}{dt} \right)^2 - a\omega^2 \cos\omega t \right) \quad (3-12)$$

The movement of particles on the wall has three possibilities[52], as follows, when $N > 0$:

1. relatively stationary compared with the wall
2. positive slip
3. negative slip

These are not so important under our experimental conditions. We could neglect the difference in these movements on the wall for the behavior of the particles. When $N < 0$, it has nothing to do with the wall.

The simulated trajectory of the particle beside the wall is shown in Fig. 3.4. Table 3.1 gives the time required for one cycle. The direction of the particle movement is opposite to the direction of circular motion.

The result of the simulated period was approximately dependent on the radius multiplied the frequency of the circular motion. Figure 3.5 shows the relationship between the average traveling rate of particles beside the wall, $D_v \pi / t$, and the velocity of circular motion, $r_T \omega$. The line was a value calculated with equation 3-7. The experimental result did not follow the line, especially in the range of the small and high velocity. However, the tendency was similar to the calculated values.

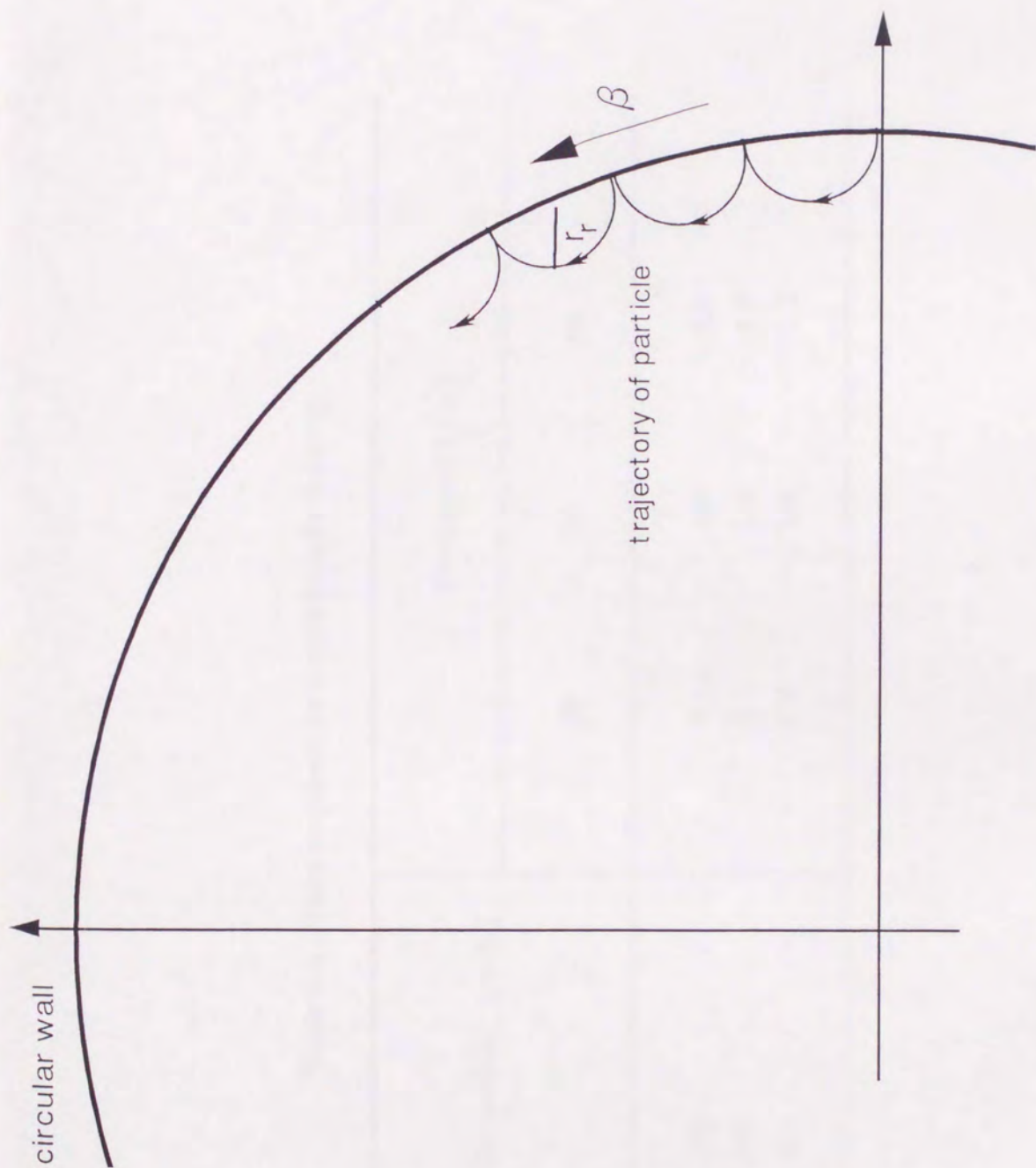


Fig. 3.4 Movement of a particle beside a wall

Table 3.1 Time required for 1 cycle beside the wall

Radius of circular motion [mm]	Frequency [1/s]		
	20	30	40
2.0	6.8s	4.0	2.9
3.0	4.2	2.4	1.8
4.0	3.0	1.8	1.3

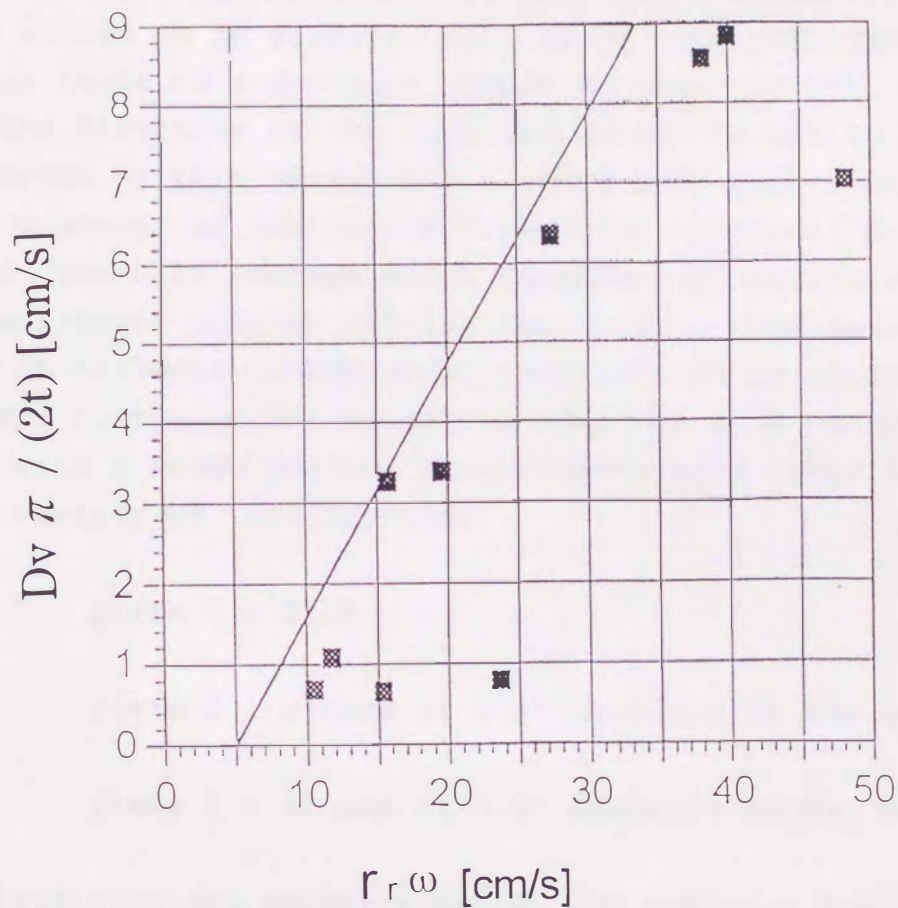


Fig.3.5 The relationship between the traveling rate of particles beside the wall and the velocity of the circular motion

3.3 Separation performance for spherical glass beads and nonspherical ground glass particle

3.3.1 EXPERIMENTAL APPARATUS AND MATERIAL

The experimental apparatus is a brass cylindrical vessel, which is 145 mm in diameter and 20 mm in depth, fixed on the shaking table of a gyratory screen as shown in Fig. 3.6.

The direction of the circular motion is set to be clockwise. The bottom of this vessel has a round hole with a collector of 60 mm in diameter at the center collecting spherical particles and a gate at the wall through which nonspherical particles are routed to a collector located outside the vessel. The gate has a scraper which collects nonspherical particles to an outside collector.

The bottom of the vessel is composed of a centerholed brass plate with a rough surface blasted with sand under 300 μm which has a variety of inclinations:

plate 1 ; flat

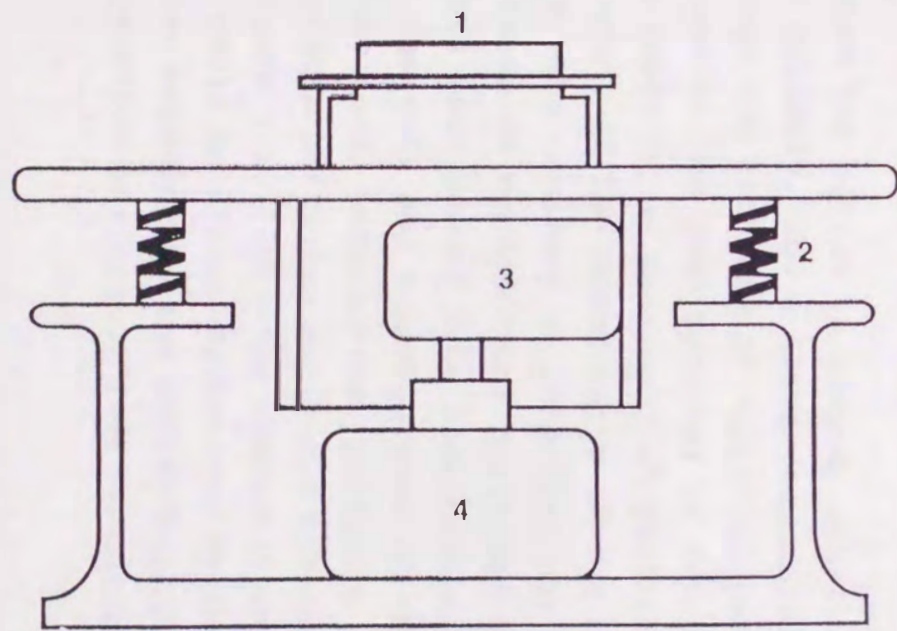
plate 2 ; sloped at 1.5° downward to the center

plate 3 ; sloped at 3.0° downward to the center

Particles are normally fed at the position just behind the gate. Spherical particles run into the central collector directly, or after bouncing against the wall, depending on the feeding direction, while nonspherical particles travel counter-clockwise along the wall. Finally, they touched the scraper and were eventually scraped out from the gate.

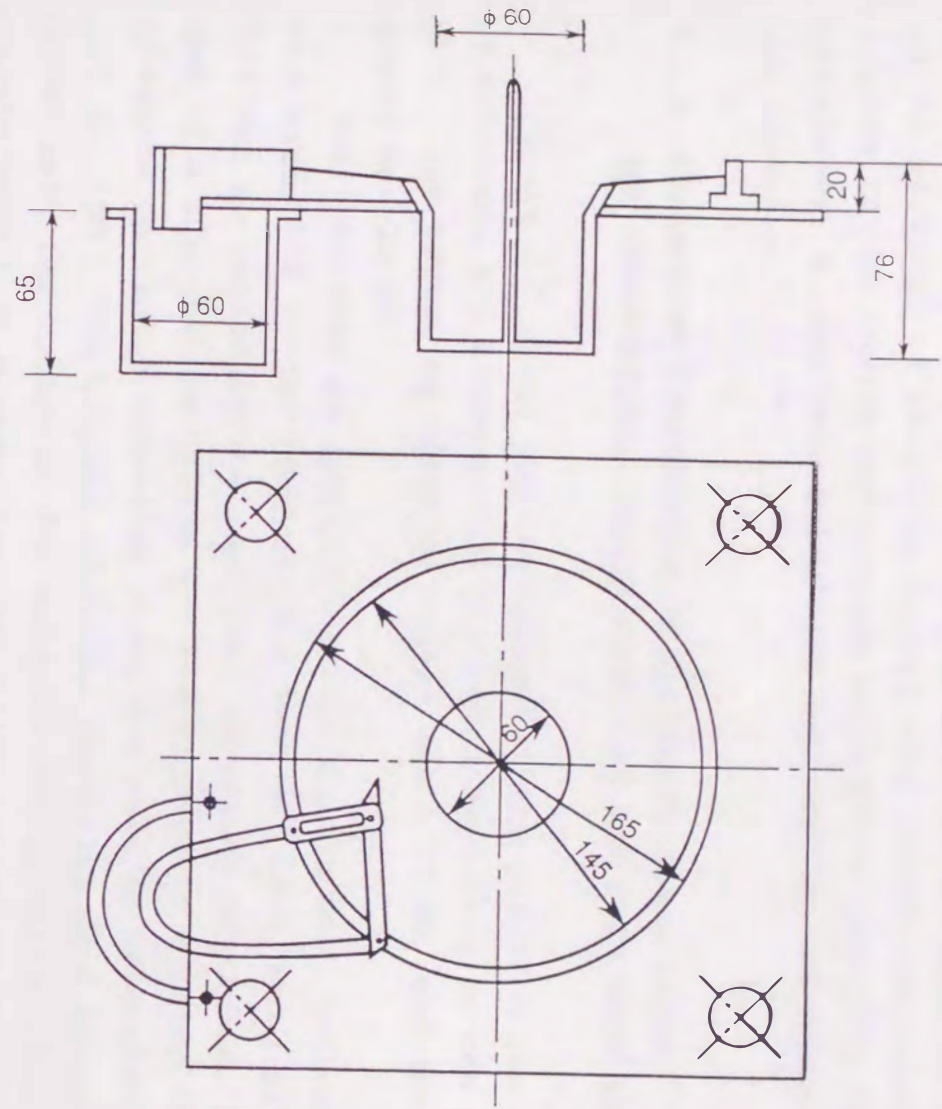
Samples for the separation test are differently proportioned artificial mixtures of ground glass sized 500 - 840 μm and glass beads sized 500 - 710 μm , which were fed by means of a vibrating feeder. The feed rate was calculated by measuring the duration required for charging a certain mass of samples.

The radius and frequency of the driving circular motion were 1.6 mm and 20 Hz, respectively. The recoveries of spherical and



- 1. Vessel
- 2. Spring
- 3. Unbalance weight
- 4. Motor

Shaking table of gyratory screen



Vessel (dimension is mm)

Fig.3.6 Horizontally circular motion plate

nonspherical particles have been determined by counting particles in the pictures of particles distributed during the separating process to the inside and outside collectors; Newton's separation efficiency, η , has been calculated followed by the equation in the Appendix.

3.3.2 SEPARATION PERFORMANCE OF SPHERICAL GLASS BEADS AND NONSPHERICAL GROUND PARTICLES FOR FEED RATE[46]

Figure 3.7 shows the influences of the plate on the recovery of spherical and nonspherical particles depending on the feed rate. The radius of circular motion was 1.58 mm, and the frequency was 20 Hz.

The recovery of spherical particles has been influenced by feed rate, and better recovery has been obtained using plate 3. This can be caused by the fact that spherical particles, in the case of a flat bottom (plate 1), are trapped in a crowd of nonspherical particles traveling along the wall as described in the last section. The trapped spherical particles were brought together into the collector for nonspherical particles when a certain amount of nonspherical particles exists on the bottom plate.

When the bottom is sloped, spherical particle can behave rather properly, and a better separation can take place. Figure 3.8 shows the recovery of spherical particles influenced by the component of the feed material at $R=1.62$ mm and $f=20$ Hz. Considerable recovery of nonspherical particles has been maintained independent of the mixed ratio of the constituents in Fig. 3.9; however, the recovery of spherical particles declined as the mixed ratio of nonspherical particles increased.

This must result from nonspherical particles being retained beside the wall and trapping some of the spherical particles. On the other hand, nonspherical particles have not been intercepted by spherical particles and could maintain their trajectories.

Figure 3.10 indicates summarily that the separation efficiency could be almost determined by the amount of nonspherical particles existing on the separating plate. It was clear that the separation efficiency (see Appendix) in Fig. 3.11 was decided

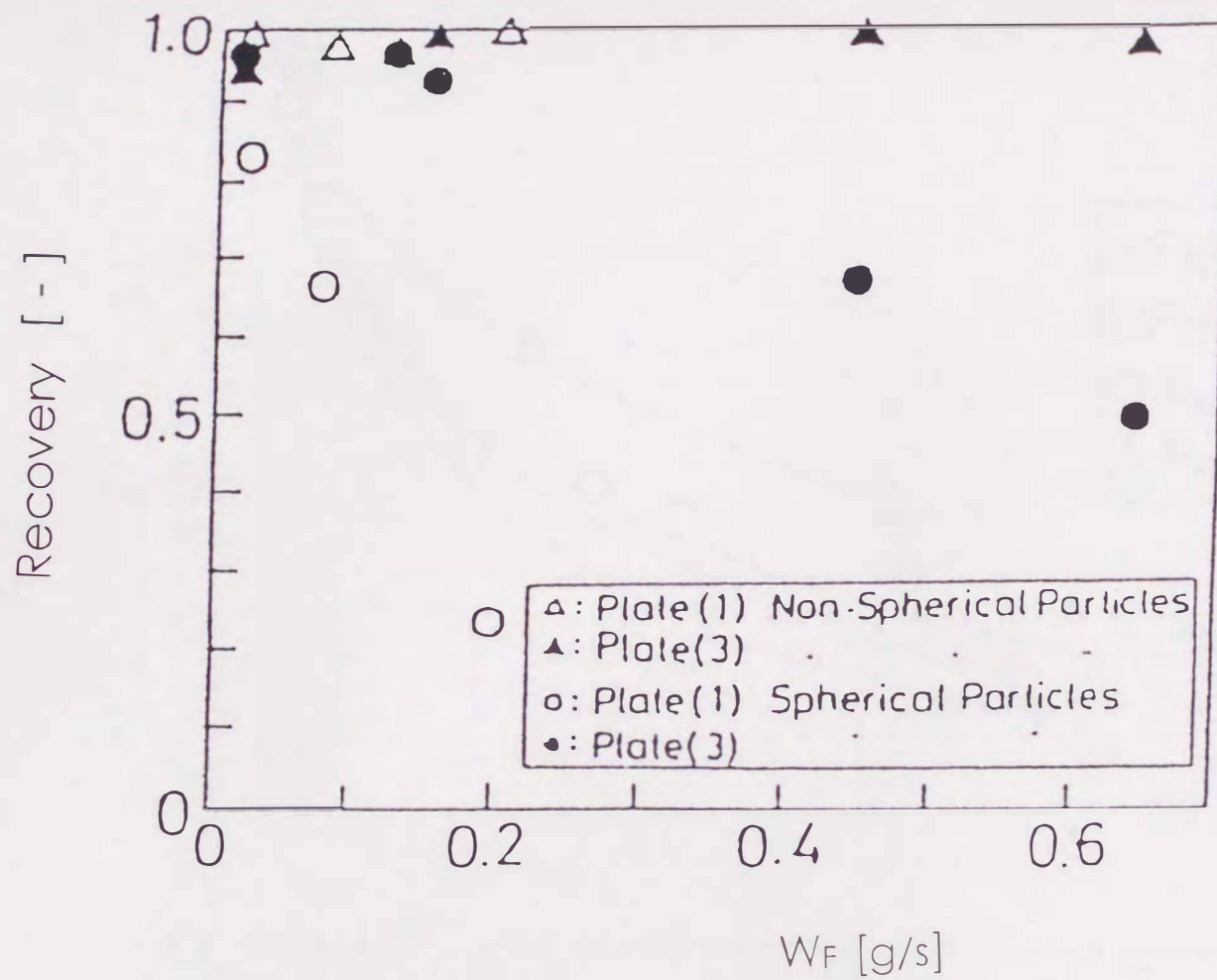


Fig.3.7 Recovery of spherical and nonspherical particles with plates 1 and 3

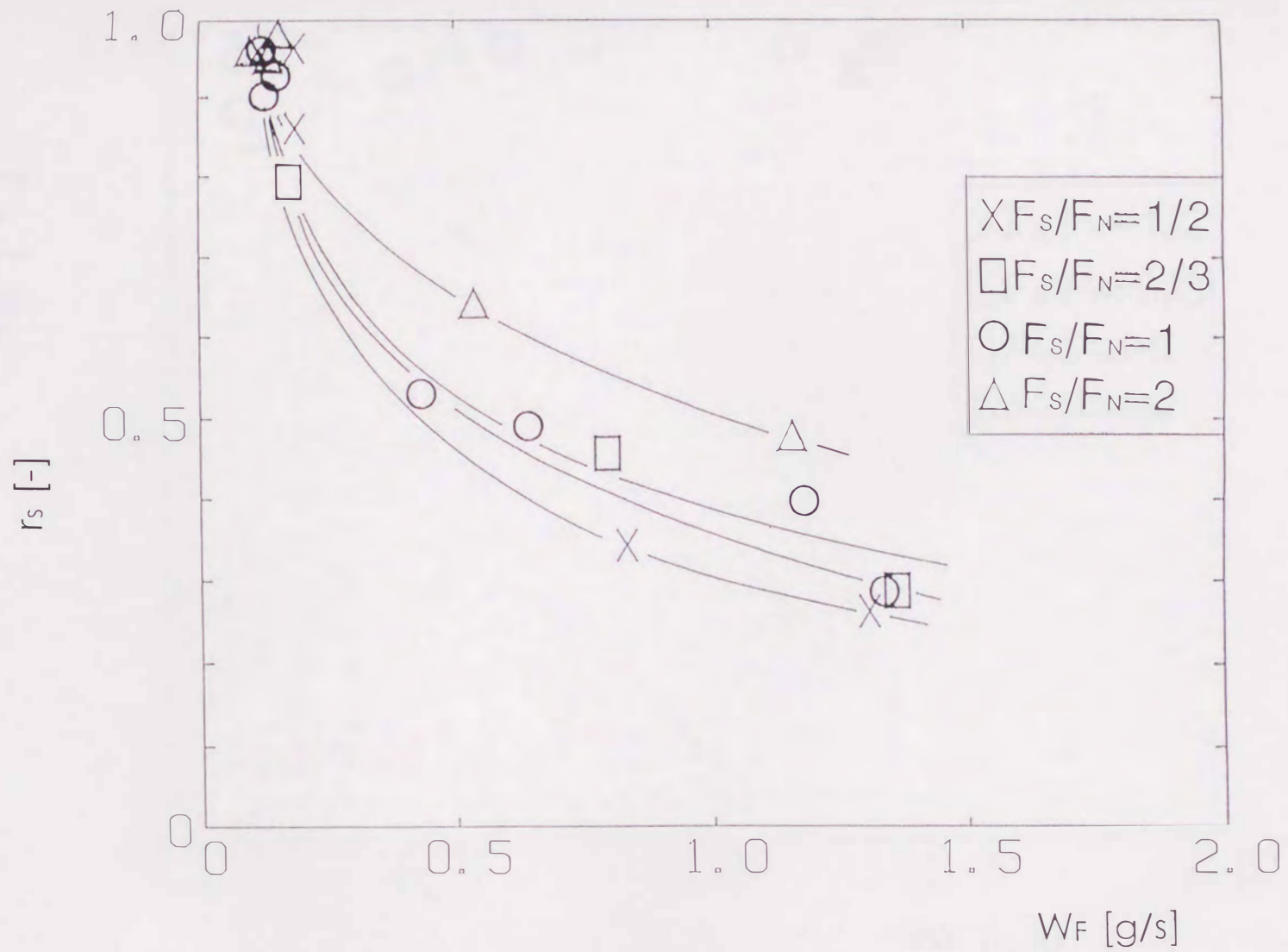


Fig.3.8 Recovery of spherical particles with 4 different mixed ratios of feed materials

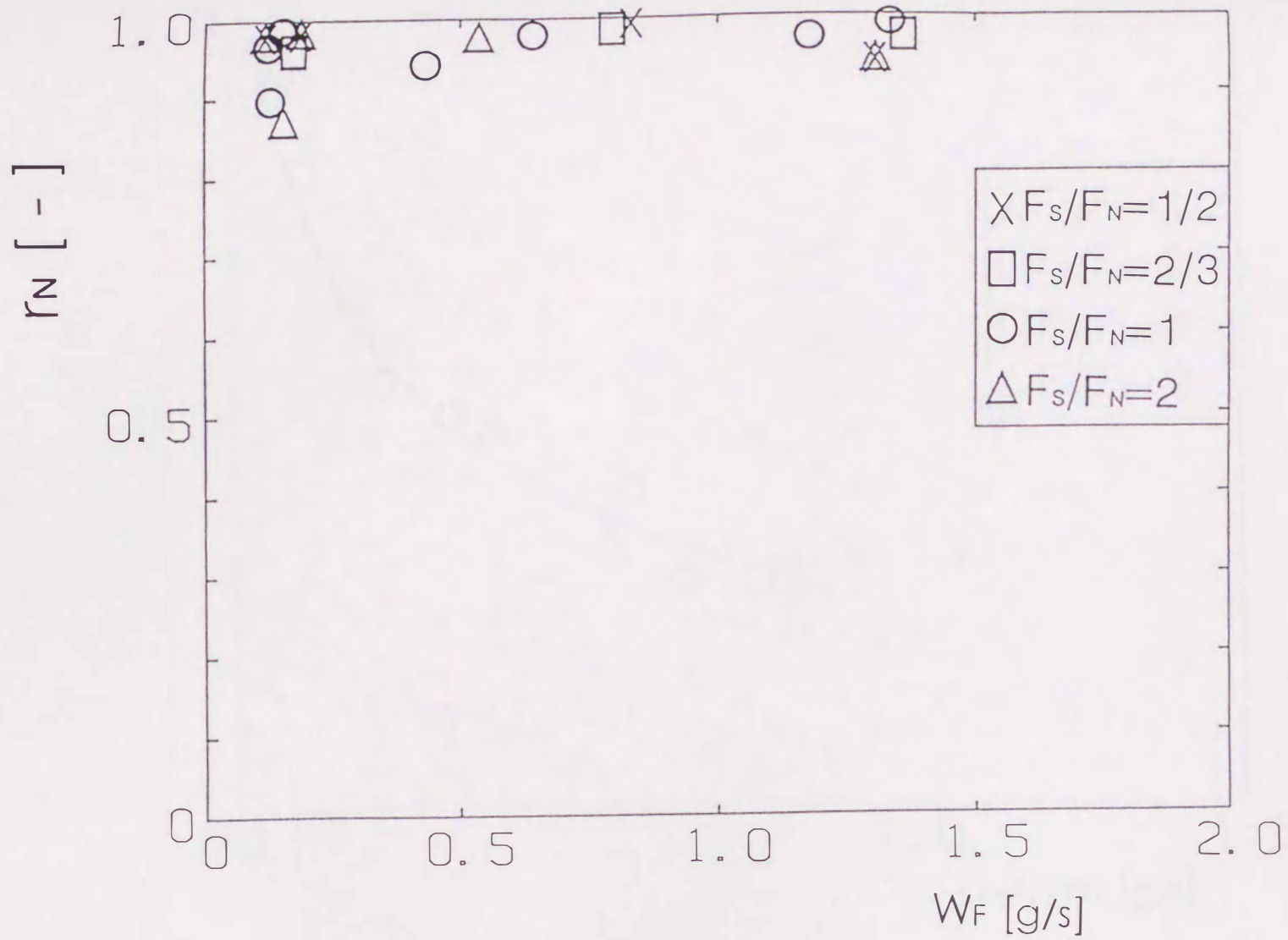


Fig.3.9 Recovery of nonspherical particles with 4 different mixed ratios of feed materials

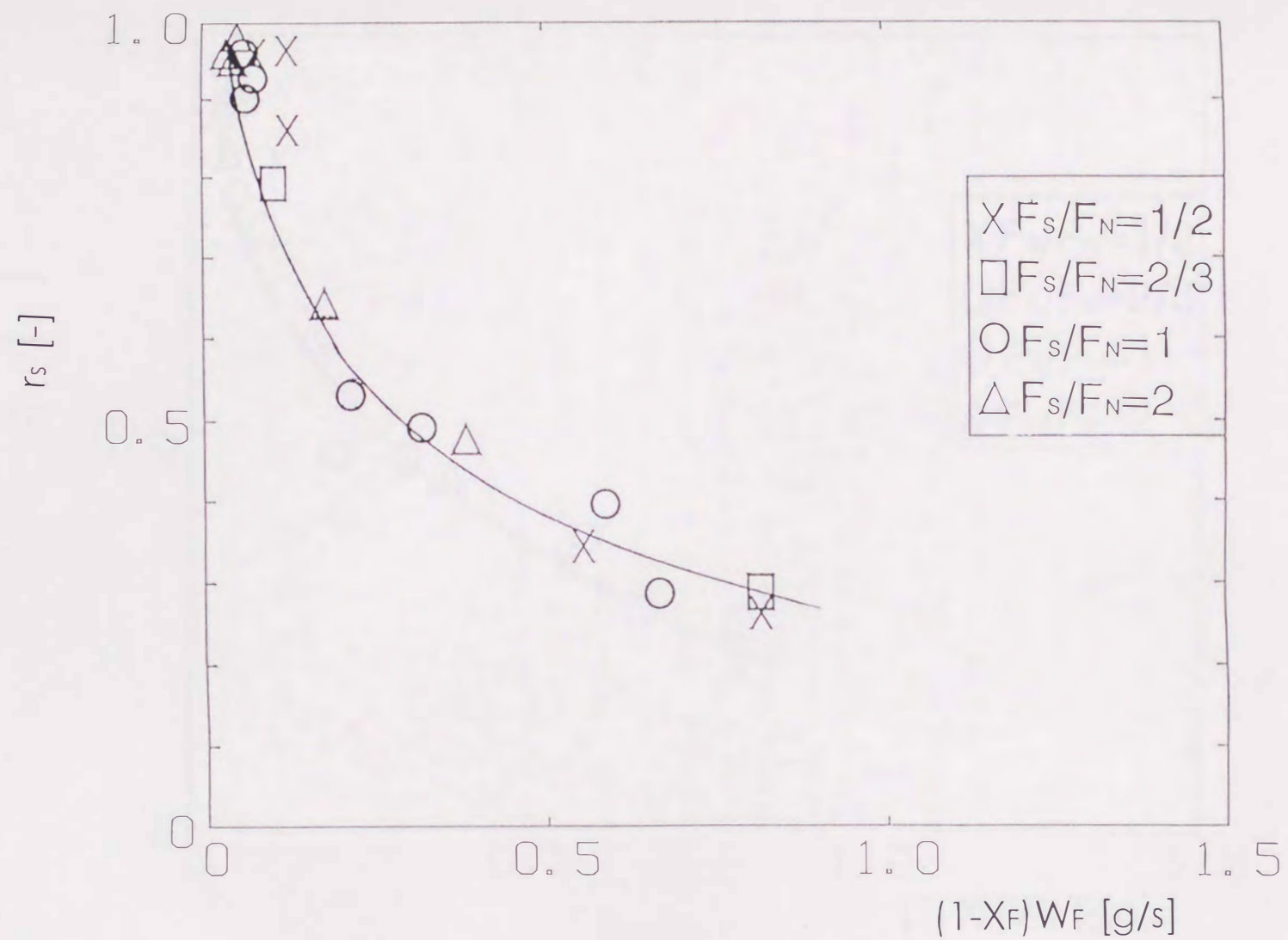


Fig.3.10 Recovery of spherical particles affected by feed rate of nonspherical particles

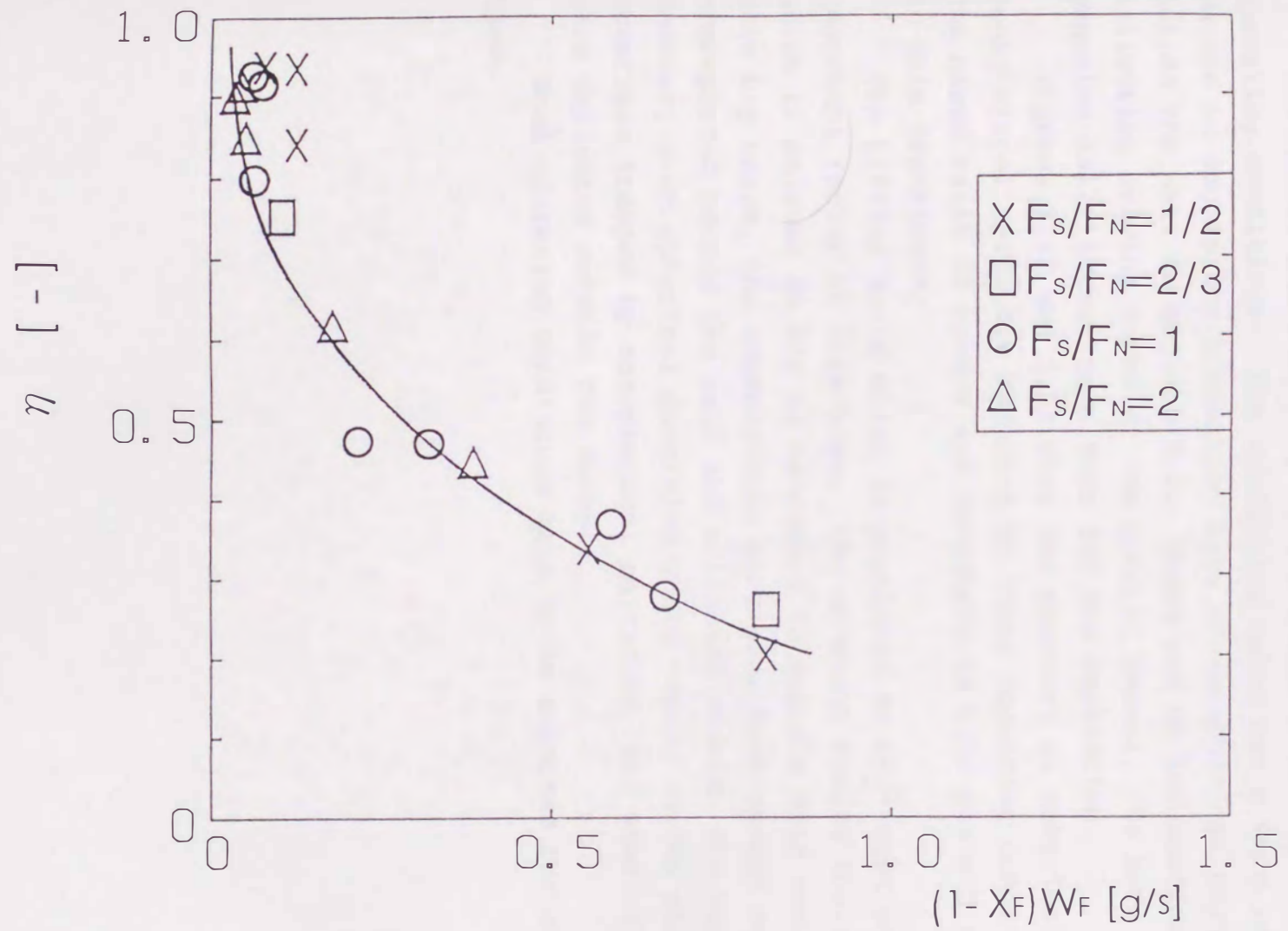


Fig.3.11 Newton's separation efficiency affected by feed rate of nonspherical particles

by the retention of the nonspherical particles on the plate.

3.3.3 EFFECT OF OPERATING CONDITIONS

The radius and frequency of the circular motion were the operating conditions. The multiplied value was a very important factor to decide the travelling rate of nonspherical particles beside the wall in section 3.2. There was no information on the collecting driving force to the central vessel. We have to experimentally investigate them for the separation.

Figures 3.12 and 3.13 show the recovery of spherical and nonspherical particles affected by these operating conditions. The mixed ratio of sphere and nonsphere is 1:1; plate 3 was used in this experiment.

The hitting force which is populated to $R \cdot f^2$ must not be an important factor at this time. The movement beside the wall which is related to $R \cdot f$ is necessary to explain this result. At this big value, the nonspherical particles have enough rate to be transported beside the wall and collected outside the vessel. However, even spherical particles would remain on the plate, sometimes trapped by nonspherical particles, and some of them were collected outside the vessel.

Good operating conditions have to be selected for any samples.

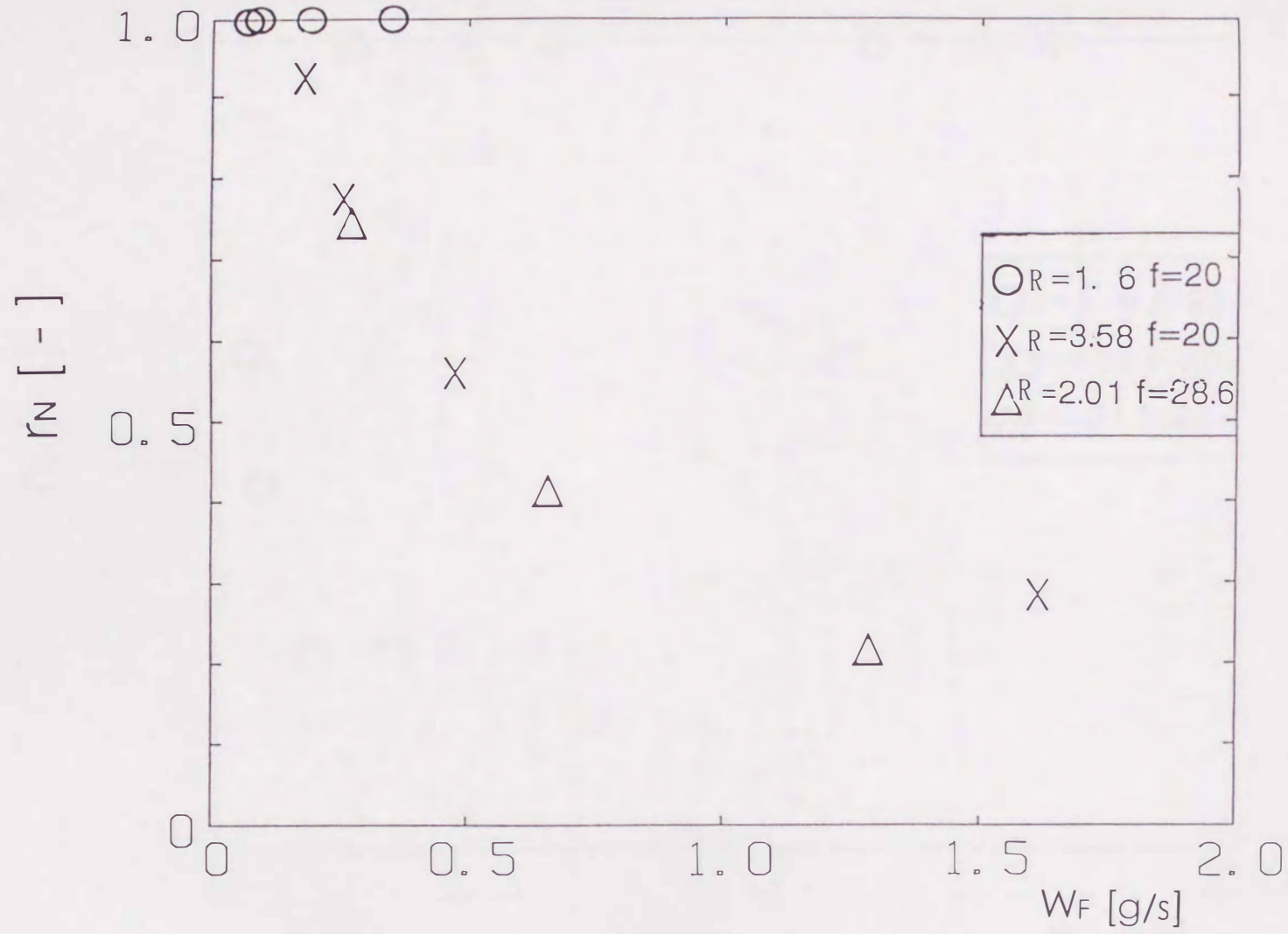


Fig.3.12 Recovery of spherical particles affected by the radius and frequency of the circular motion

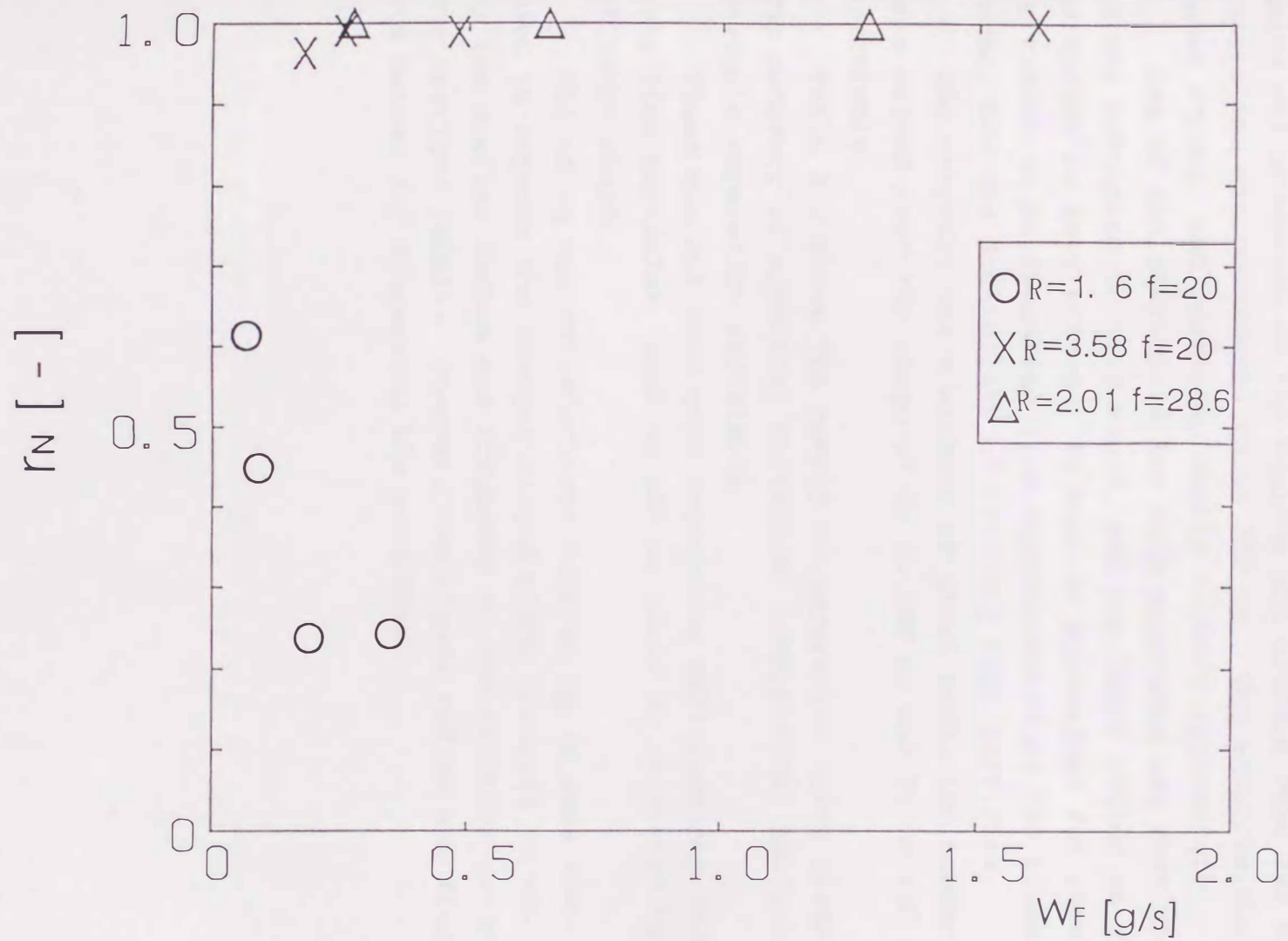


Fig.3.13 Recovery of nonspherical particles affected by the aradius and frequency of the circular motion

3.4 Shape separation for fine particles

Generally speaking, the lower limit of the particle size which was processed on the rolling and sliding type for shape separation was considered to be 300 μm . The adhesive force becomes strong, and particles easily tightly agglomerate.

One of the characters for this apparatus was that the motion of the particles is very rapid, and the force acting on the particles is very strong. It must be convenient for adhesive particles to be dispersed from agglomeration on the plate. This method has the possibility of treating fine particles.

The material was a mixture of glass beads and powders, which were sieved over the range of 90 to 159 μm and 74 to 150 μm , respectively.

Table 3.2 shows the result of separation using plate 3 for the recovery of spherical particles, nonspherical particles and Newton's separation efficiency.

These are not such good separation efficiencies; however, very fine particles, such as 100 μm could be separated by means of their shape.

All of r_N was satisfactory; however r_S is less than 0.5. We have to improve the steeper-sloped plate downward to the center or the smaller radius and frequency of the circular motion for the previous result. However, the bigger radius and frequency are better for dispersing the particles.

Table 3.2 r_s, r_N, η for fine particles

	Radius of circular motion: R [mm]	frequency: f [Hz]	r_s	r_N	η
1	2.70	16.67	0.446	0.995	0.441
2	2.75	22.50	0.007	1.000	0.007
3	3.60	16.67	0.021	0.996	0.017
4	1.89	16.67	0.244	0.989	0.233

3.5 Distinction of nonspherical particles

The distinction between two kinds of materials, which have almost the same size ranging from 298 to 840 μm , was performed. The samples used are weathered quartz from the Philippines which has a slightly rounded shape with a smooth surface, called sample A (white); ground quartz by a cone crusher, called sample B (white); and a slag from the Japanese iron works, prepared by grinding featuring a cornered shape with relatively rough surface, called sample C (gray), as shown in the photographs in Fig. 3.14.

There was a distinct difference in the particle shape among the three samples, in particular A from B and C. However, the difference is subtle compared with the difference between the spherical and nonspherical particles.

Table 3.2 is a characterization of the particles. Both mixed samples had the same mass of the individual samples. Plate 2 has been used for this experiment. As for the driving circular motion, the radius was fixed at 2.25 mm, and the frequency was varied from 20 Hz to 31 Hz. The vertical vibration accompanied with horizontally circular motion has been observed to have the same frequency as that of the horizontal motion and the amplitude was 0.4 mm.

Figures 3.15 and 3.16 show at the top the recovery of sample A collected in the central vessel and that of sample B or C collected outside, depending on the frequency of vibration, where both samples were fed separately and the feed rate was set to be slow enough so as to make the particles behave as properly as possible[53].

The amount of particle collected in the center increased with the frequency, independent of sample. It did not agree with the results of the separation between the spherical and nonspherical particles in section 3.3. The hitting force to the particles by the wall had to be more important because of the gentler slope.

The collected directions of the particles in these diagrams were considerable between the two nonspherical materials, the

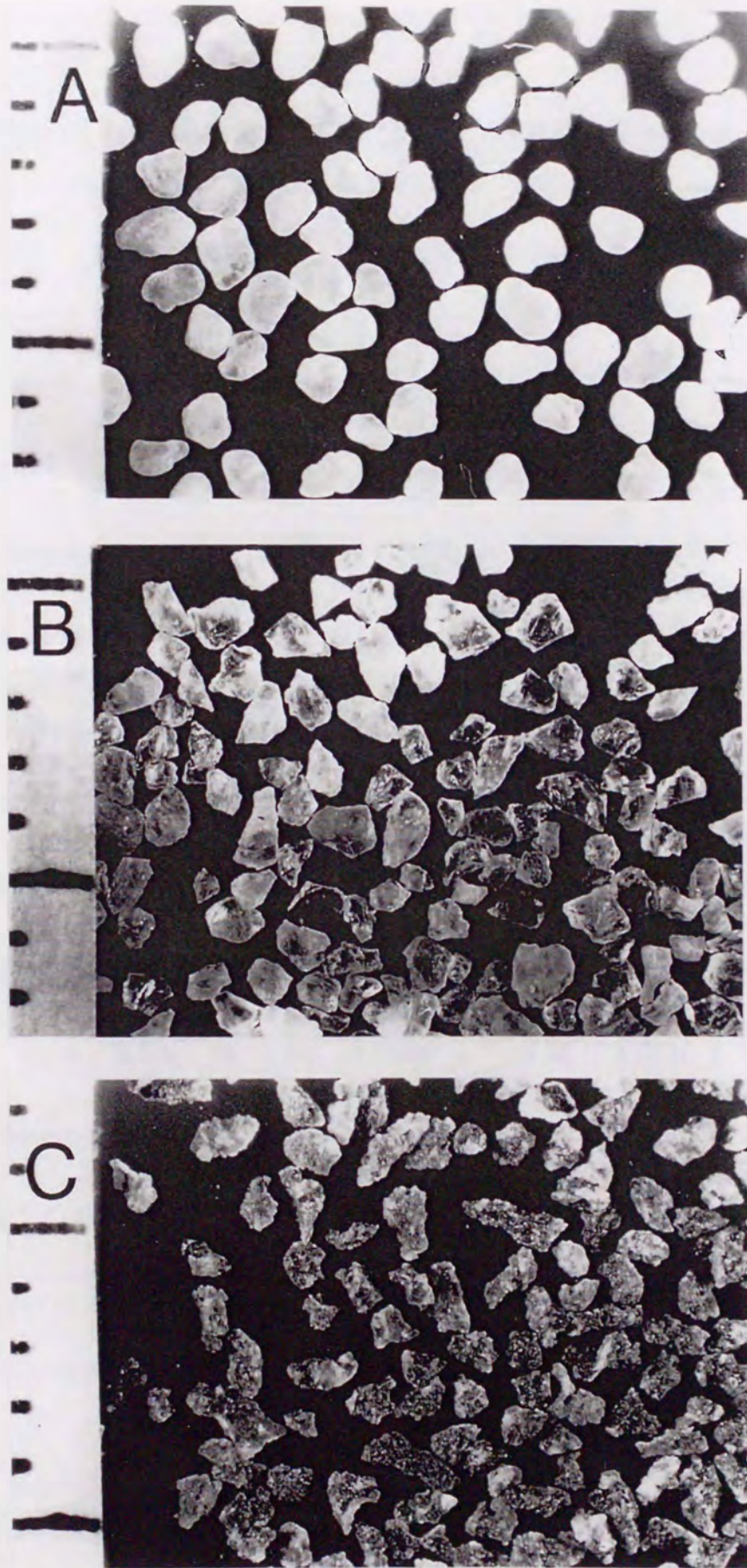


Fig.3.14 Photographs of weathered quartz, ground quartz and slugs

Table 3.3 Characterization of silica, grinding silica, slug

	A quartz	B ground quartz	C slug
perimeter [mm]	2.47 = 0.28	2.56 = 0.50	2.77 = 0.56
area of [mm ²]	0.576 = 0.111	0.474 = 0.171	0.494 = 0.162
degree of circularity [-]	0.954 = 0.033	0.890 = 0.068	0.806 = 0.095
Heywood diameter [mm]	0.85 = 0.08	0.77 = 0.14	0.73 = 0.12
horizontal Feret diameter [mm]	0.90 = 0.13	0.83 = 0.13	0.90 = 0.26
vertical Feret diameter [mm]	0.87 = 0.12	0.82 = 0.19	0.86 = 0.21
maximum diameter [mm]	1.03 = 0.11	0.98 = 0.20	1.03 = 0.25
shape factor [-]	1.480 = 0.178	1.646 = 0.247	1.339 = 0.405
major factor [mm]	0.94 = 0.13	0.39 = 0.21	1.00 = 0.25
minor axis [mm]	0.76 = 0.10	0.66 = 0.12	0.66 = 0.12
shape factor 2 [-]	0.809 = 0.044	0.791 = 0.045	0.745 = 0.055

$$\text{shape factor 1} = \frac{(\text{maximum diameter})^2}{\text{projected area}} \times \frac{\pi}{4}$$

$$\text{shape factor 2} = \frac{\text{projected area}}{\text{major axis} \times \text{minor axis}} \times \frac{\pi}{4}$$

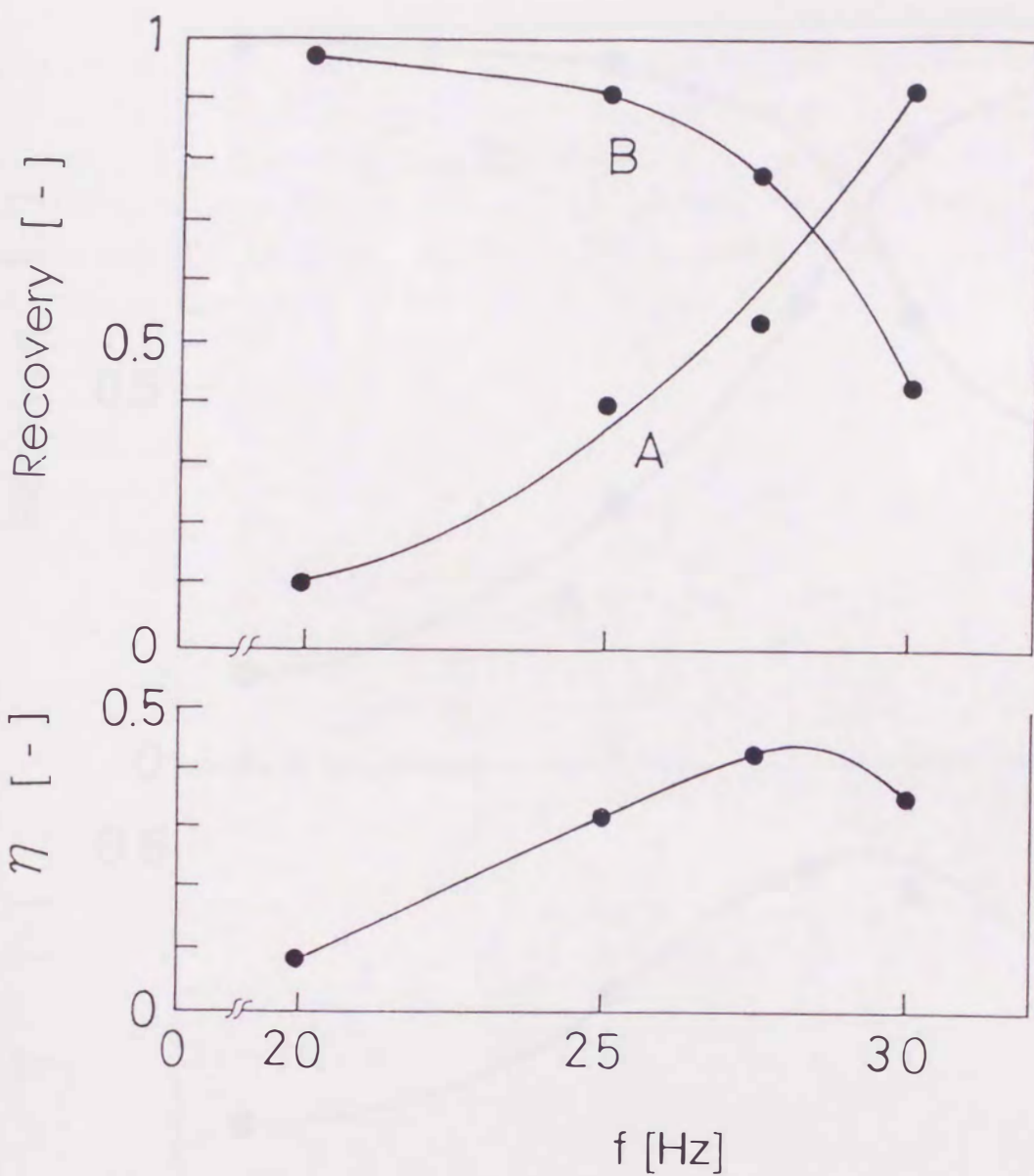


Fig.3.15 Recovery of spherical and nonspherical particles and Newton's separation efficiency affected by the frequency of the vibration

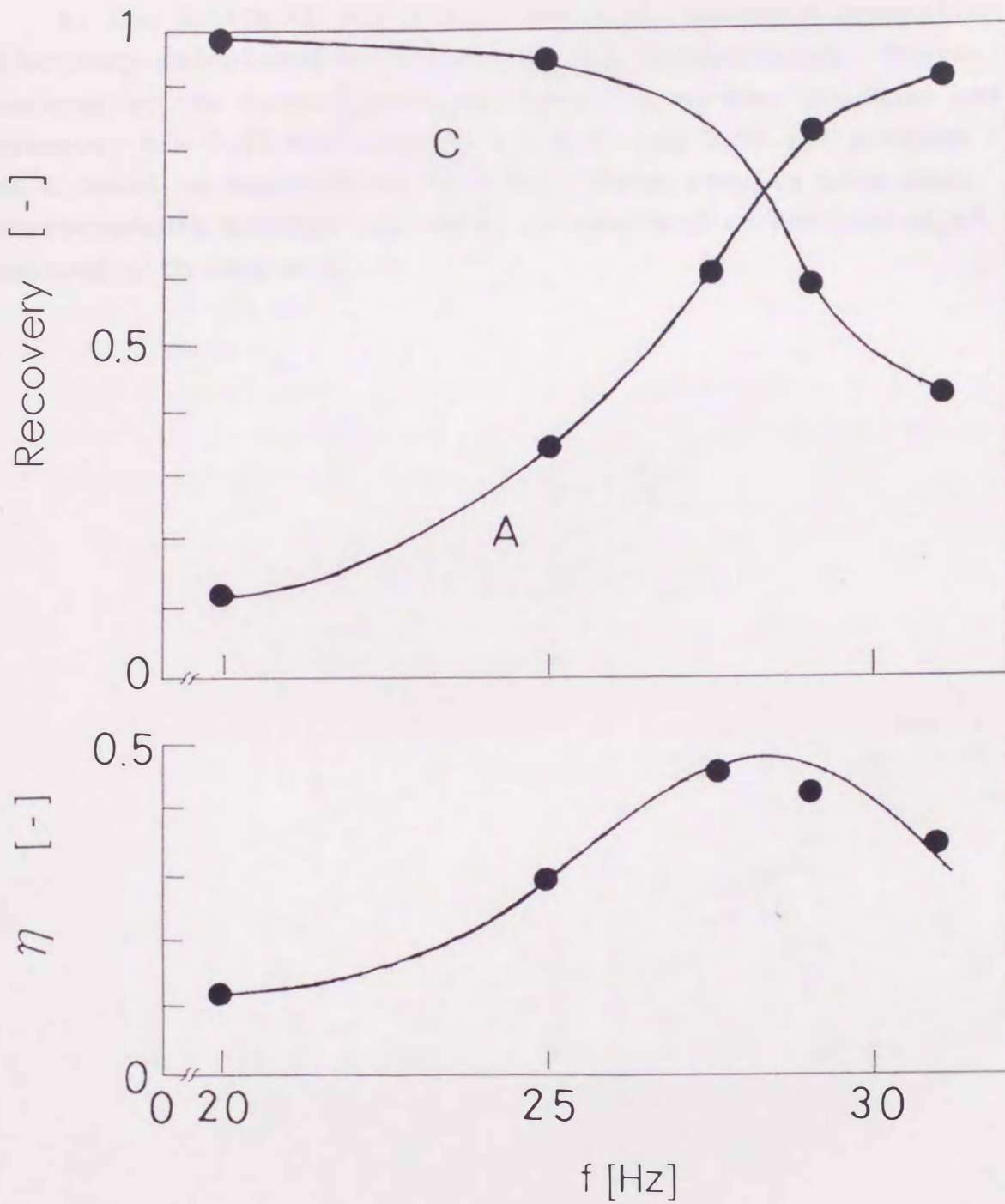


Fig.3.16 Recovery of spherical and nonspherical particles and Newton's separation efficiency affected by the frequency of the vibration

round-edged particle of sample A to the central vessel and the sharper-edged particle of sample B or C to the outside vessel.

At the bottom of Fig.s 3.15 and 3.16, Newton's separation efficiency calculated from the Appendix is indicated. Corresponding to the intersection of the above curves, the best performance, $\eta = 0.45$ for samples A and B, and 0.50 for samples A and C could be expected at 28.6 Hz. These results were also understandable because the shape of sample C is sharper-edged compared with sample B.

3.6 Conclusions

The motion of particles on the infinite plate which moves circularly was analyzed by the kinetic equations. We presented the model of particle motion beside the circular wall on the horizontally circular motion.

we could separate the spherical glass beads from nonspherical ground glass particles. The recovery of nonspherical particles declined as the feed rate of the nonspherical particles. This resulted from nonspherical particles retained beside the wall and trapping some of the spherical particles.

The separation of fine particles and the distinction of nonspherical particles were also performed.